

Chapter 10. Radiation by Relativistic Charges

In this chapter, I return to EM wave radiation by moving charges, because the relativity background of the previous chapter will allow us to analyze these effects for arbitrary speed of the radiating particle. After analysis of such important particular cases as synchrotron radiation and “Bremsstrahlung” (brake radiation), I will discuss the apparently unrelated effect of Coulomb losses, which nevertheless will lead us to such important phenomena as the Cherenkov radiation and transitional radiation. In the end of the chapter I will briefly discuss the effects of back action of the emitted EM radiation on the charged particle which emits it, and in this context mention the limits of classical electrodynamics.

10.1. Liénard-Wiechert potentials

The starting point for the discussion of radiation by moving charges is provided by Eqs. (8.17) for retarded potentials. In free space these formulas look as

$$\phi(\mathbf{r}, t) = \frac{1}{4\pi\epsilon_0} \int \frac{\rho(\mathbf{r}', t - R/c)}{R} d^3r', \quad \mathbf{A}(\mathbf{r}, t) = \frac{\mu_0}{4\pi} \int \frac{\mathbf{j}(\mathbf{r}', t - R/c)}{R} d^3r'. \quad (10.1)$$

Here R is the magnitude of the vector,

$$\mathbf{R} = \mathbf{r} - \mathbf{r}', \quad (10.2)$$

which connects the source point \mathbf{r}' to the observation point \mathbf{r} . As a reminder, Eqs. (1) were derived from the Maxwell equations without any restrictions, and are very convenient for situations with continuous distribution of charge and current. However, for point charges, with delta-functional ρ and \mathbf{j} , it is more convenient to recast them into a different form which would not require integration over the \mathbf{r}' space.

Naively, one could suggest the following apparent (but wrong) reduction of Eqs. (1) for the point charge q moving with velocity \mathbf{u} :

$$\phi = \frac{1}{4\pi\epsilon_0} \frac{q}{R}, \quad \text{i.e.} \quad \frac{\phi}{c} = \frac{\mu_0 qc}{4\pi R}, \quad \mathbf{A} = \frac{\mu_0 q\mathbf{u}}{4\pi R}, \quad \text{(WRONG!)} \quad (10.3)$$

This is a good example how the science of relativity (even special :-)) cannot be taken too lightly. Indeed, the 4-vector (9.84) formed from potentials (3) would not obey the Lorentz transform rule (9.91), because distance R also depends on the reference frame it is measured in.

In order to correct the error, we need, first of all, to specify what exactly is R for a point charge. Evidently, in this case, only one space-time point $\{\mathbf{r}', t'\}$ may contribute to integrals (1) for any observation point $\{\mathbf{r}, t\}$. The point should be found from equation $t' = t - R/c$, i.e.

$$c(t - t') = |\mathbf{r}(t) - \mathbf{r}(t')|. \quad (10.4)$$

Figure 1 depicts the graphical solution of this self-consistency equation as the point of intersection of the light cone of the observation point (see Fig. 9.9 and its discussion) and the trajectory of the charged particle. (Formally, there is always another point $\{\mathbf{r}'', t''\}$, with $t'' > t$, which is also a solution to this equation, but it should be ignored on the basis of causality arguments.) Let us give index “ret” to all

variables corresponding to the retarded solution $\{\mathbf{r}', t'\}$ of Eq. (4) e.g., $c(t - t') \equiv R_{\text{ret}}$ (Fig. 1), $\mathbf{u}\{\mathbf{r}', t'\} \equiv \mathbf{u}_{\text{ret}}$, etc, as measured in the “lab” reference frame (generally, the inertial frame moving with the observation point).

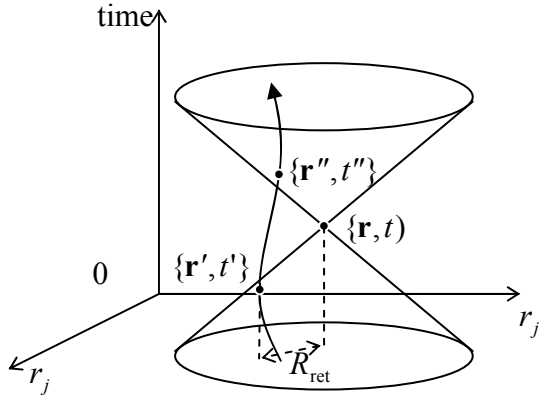


Fig. 10.1. Graphical solution of Eq. (3).

Now, let us write Eqs. (1) for a point charge in an inertial reference frame which has, and the moment t' under consideration, the same velocity (\mathbf{u}_{ret}) as the charge. In that frame, the particle rests, and the evident integration yields

$$\phi = \frac{q}{4\pi\epsilon_0|\mathbf{r} - \mathbf{r}'|} = \frac{q}{4\pi\epsilon_0 R}, \quad \mathbf{A} = 0, \quad (10.5)$$

but let us remember that this R may not be equal to R_{ret} in our definition, because the latter distance is measured in the “lab” reference frame. Let us rewrite Eq. (5) in the form of components of a 4-vector similar in structure to Eq. (3):

$$\frac{\phi}{c} = \frac{\mu_0}{4\pi} q \frac{c}{R}, \quad \mathbf{A} = 0. \quad (10.6)$$

Now it is easy to guess the correct answer for the whole 4-potential:

$$A^\alpha = \frac{\mu_0}{4\pi} q \frac{cu^\alpha}{u_\beta R^\beta}, \quad (10.7)$$

where (as a reminder), $A^\alpha \equiv (\phi/c, \mathbf{A})$, $u^\alpha \equiv \gamma\{c, \mathbf{u}\}$,¹ and R^α is also a 4-vector formed similarly to that of a single world event – cf. Eq. (9.48):

$$R^\alpha \equiv \{c(t - t'), \mathbf{R}\} \equiv \{c(t - t'), \mathbf{r} - \mathbf{r}'\}. \quad (10.8)$$

Indeed, we need A^α which would: (i) obey the Lorentz transform, (ii) have its spatial components A_j scaling as u_j , and (iii) be reduced to the correct result (5) in the reference frame moving with the

¹ From this point on, I will drop index u in what was called γ_u in Chapter 9, because in what follows there will be hardly any chance to confuse particle’s velocity u with a reference frame velocity v . Hence, in all formulas below $\gamma \equiv 1/(1 - u^2/c^2)^{1/2} = 1/(1 - \beta^2)^{1/2}$. Also, note the following relations: $\gamma^2 = 1/(1 - \beta^2)$ and $(\gamma^2 - 1) = \beta^2/(1 - \beta^2) = \gamma^2\beta^2$, which are very handy for the relativity-related algebra.

charge. Equation (7) evidently satisfies all these requirements, because the scalar product in its denominator is just

$$u_{\beta} R^{\beta} = \gamma \{c, -\mathbf{u}\} \cdot \{c(t-t'), \mathbf{R}\} = \gamma [c^2(t-t') - \mathbf{u} \cdot \mathbf{R}] = \gamma c(R - \boldsymbol{\beta} \cdot \mathbf{R}) = \gamma cR(1 - \boldsymbol{\beta} \cdot \mathbf{n}), \quad (10.9)$$

where $\boldsymbol{\beta} \equiv \mathbf{u}/c$ is the normalized velocity of the particle, and $\mathbf{n} \equiv \mathbf{R}/R$ is a unit vector in the observer's direction. In the reference frame of the charge (where $\boldsymbol{\beta} = 0$), the denominator is reduced to cR , correctly reducing Eq. (7) to Eq. (6). Now let us spell out components of Eq. (7) in the lab frame (where $R = R_{\text{ret}}$):

$$\phi = \frac{1}{4\pi\epsilon_0} \frac{q}{(R - \boldsymbol{\beta} \cdot \mathbf{R})_{\text{ret}}} = \frac{1}{4\pi\epsilon_0} q \left(\frac{1}{R(1 - \boldsymbol{\beta} \cdot \mathbf{n})_{\text{ret}}} \right), \quad (10.10a)$$

$$\mathbf{A} = \frac{\mu_0}{4\pi} q \left(\frac{\mathbf{u}}{R - \boldsymbol{\beta} \cdot \mathbf{R}} \right)_{\text{ret}} = \frac{\mu_0}{4\pi} qc \left(\frac{\boldsymbol{\beta}}{R(1 - \boldsymbol{\beta} \cdot \mathbf{n})_{\text{ret}}} \right) = \phi \frac{\mathbf{u}_{\text{ret}}}{c^2}. \quad (10.10b)$$

These formulas are called the *Liénard-Wiechert potentials*.² In the nonrelativistic limit, they are equivalent to our first guess (4), but include a denominator which describe the change of the effective charge of the source due to the apparent change of distance R , at $\beta \sim 1$. In order to understand its origin, let us consider a simple 1D model when a charged rod, of length l , moves directly toward the observer (Fig. 2).

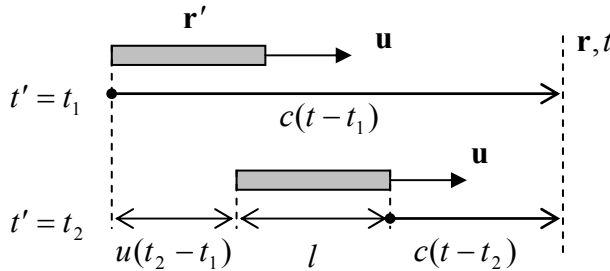


Fig. 10.2. The geometrical effect behind factor $(1 - \boldsymbol{\beta} \cdot \mathbf{n})$ in denominator of the Liénard-Wiechert potentials.

Since speed u cannot exceed the speed of light c , in order to reach the observer at the same moment t , EM radiation from the far end of the rod should leave the source earlier (at moment $t' = t_1$) than that from its closer end (at $t' = t_2 > t_1$). However, during this time interval the rod has moved by distance $u(t_2 - t_1)$ – see the lower panel in Fig. 2. From the evident distance balance,

$$c(t - t_1) = u(t_2 - t_1) + l + c(t - t_2), \quad (10.11)$$

we see that regardless of t (i.e. the observer's position), the time interval between the radiation events,

$$\Delta t' \equiv t_2 - t_1 = \frac{l}{c - u} = \frac{\Delta t}{1 - \beta}, \quad (10.12)$$

is a factor of $1/(1 - \beta)$ smaller than what it would be ($\Delta t = l/c$) at negligible source speed. Due to this time compression,³ the apparent charge density is correspondingly higher, in agreement with Eq. (10), in which for our simple case we should take $\boldsymbol{\beta} \cdot \mathbf{n} = \beta$.

² These formulas were derived in 1898 by A.-M. Liénard and, independently, in 1900 by E. Wiechert.

³ Note that this time compression effect (linear in β) has nothing to do with the Lorentz time dilation (because all our arguments refer to the same, lab frame), but is closely related to the Doppler effect.

So, the charge re-normalization in the Liénard-Wiechert potentials is a simple geometric phenomenon which is (somewhat counter-intuitively) independent on the source size l , and hence takes place even in the limit $l \rightarrow 0$, e.g., for a point source. Here, as we have seen, the 4-vector formalism has provided a big help for the quantitative description of this effect.

Now, the electric and magnetic field corresponding to the Liénard-Wiechert result may be found by the plugging Eqs. (10) into the general formulas (6.98).⁴ This operation should be performed carefully, because Eqs. (6.98) require the differentiation over the coordinates $\{\mathbf{r}, t\}$ of the observation point, while we want the result to be expressed via particle's velocity $\mathbf{u}_{\text{ret}} \equiv (d\mathbf{r}'/dt')_{\text{ret}}$ which participates in Eqs. (10). In order to find the relation between derivatives over t and t' , let us differentiate Eq. (4), rewritten as

$$R_{\text{ret}} = c(t - t'), \quad (10.13)$$

over t and t' . In order to calculate derivative $\partial R_{\text{ret}}/\partial t'$, let us differentiate both sides of identity $R^2 = \mathbf{R} \cdot \mathbf{R}$ (for brevity, I will omit index “ret” for a while):

$$2R \frac{\partial R}{\partial t'} = 2\mathbf{R} \cdot \frac{\partial \mathbf{R}}{\partial t'}. \quad (10.14)$$

Since $\partial \mathbf{R}/\partial t' = \partial(\mathbf{r} - \mathbf{r}')/\partial t' = -\partial \mathbf{r}'/\partial t' = -\mathbf{u}$, Eq. (14) yields

$$\frac{\partial R}{\partial t'} = \frac{\mathbf{R}}{R} \cdot \frac{\partial \mathbf{R}}{\partial t'} = -\mathbf{n} \cdot \mathbf{u}. \quad (10.15)$$

Now let us differentiate the same function R over t , keeping \mathbf{r} fixed. On one hand, Eq. (13) yields

$$\frac{\partial R}{\partial t} = c - c \frac{\partial t'}{\partial t}. \quad (10.16)$$

On the other hand, according to Eq. (4), if \mathbf{r} is fixed, t' is a function of t alone, so that, using Eq. (15), we have

$$\frac{\partial R}{\partial t} = \frac{\partial R}{\partial t'} \frac{\partial t'}{\partial t} = -\mathbf{n} \cdot \mathbf{u} \frac{\partial t'}{\partial t}. \quad (10.17)$$

Requiring Eqs. (16) and (17) to give the same result, we get

$$\frac{\partial t'}{\partial t} = \frac{c}{(c - \mathbf{n} \cdot \mathbf{u})} = \frac{1}{1 - \boldsymbol{\beta} \cdot \mathbf{n}}. \quad (10.18)$$

Notice that this is the same factor which participates in the Liénard-Wiechert potentials (10) and Eq. (12), but in our current context, its another interpretation is perhaps more relevant. At fixed \mathbf{r} , the variation ∂t of the observation time corresponds to a small vertical shift of the light cone in Fig. 2, while $\partial t'$ is the corresponding shift of the retarded time t' , i.e. of the point where the world line $\mathbf{r}'(t')$ crosses the light cone of the observation point $\mathbf{r}(t)$. It is evident from that figure that if the particle does not

⁴ An alternative way to derive Eqs. (20) is to plug Eq. (7) into Eq. (9.124) to calculate the field strength tensor,

$$F^{\alpha\beta} = \frac{\mu_0 q}{4\pi} \frac{1}{u_\gamma R^\gamma} \frac{d}{d\tau} \left[\frac{R^\alpha u^\beta - R^\beta u^\alpha}{u_\delta R^\delta} \right],$$

and then spell out its components, identifying them with fields components, using Eq. (9.125).

move (i.e. its world trajectory in a vertical straight line), then $\partial t' = \partial t$. On the other hand, if the particles moves fast (with speed $u \approx c$) toward the observation point, its world line crosses the light cone at a small (“grazing”) angle, so that $\partial t' \gg \partial t$, in accordance with Eq. (18).

Since the retarded time t' , as the solution of Eq. (3), depends not only on the observation time t , but also the observation point \mathbf{r} , so we also need to calculate its corresponding derivative (gradient in \mathbf{r} -space). A calculation, absolutely similar to that carried above, yields

$$\nabla t' = -\frac{\mathbf{n}}{c(1-\boldsymbol{\beta} \cdot \mathbf{n})}. \quad (10.19)$$

Using Eqs. (18) and (19), the calculation of fields is straightforward but tedious, and I present only its result:

$$\mathbf{E} = \frac{q}{4\pi\epsilon_0} \left[\frac{\mathbf{n} - \boldsymbol{\beta}}{\gamma^2 (1 - \boldsymbol{\beta} \cdot \mathbf{n})^3 R^2} + \frac{\mathbf{n} \times \{(\mathbf{n} - \boldsymbol{\beta}) \times \dot{\boldsymbol{\beta}}\}}{(1 - \boldsymbol{\beta} \cdot \mathbf{n})^3 cR} \right]_{\text{ret}}. \quad (10.20a)$$

The only good news about this uncomfortably bulky result is that a similar differentiation gives essentially the same result for the magnetic field:

$$\mathbf{B} = \mathbf{n}_{\text{ret}} \times \frac{\mathbf{E}}{c}, \quad \text{i.e. } \mathbf{H} = \frac{1}{Z_0} \mathbf{n}_{\text{ret}} \times \mathbf{E}. \quad (10.20b)$$

Thus the magnetic and electric fields are always perpendicular to each other, and related just as in a plane wave – cf. Eq. (7.6),⁵ with the only difference that now vector \mathbf{n}_{ret} may a function of time.

As a sanity check, let us use Eq. (20a) as an alternative way to find the electric of a charge moving without acceleration, i.e. uniformly, along a straight line – see Fig. 9.11 and its discussion. (This solution will also exhibit the challenges of practical application of the Liénard-Wiechert formulas.) In this case vector $\boldsymbol{\beta}$ does not change in time, so that the second term in Eq. (20a) vanishes, so that all we need is to spell out Cartesian components of the first term. Let us select the coordinate axes and time origin in the way shown in Fig. 9.11 (see Fig. 3), and make a clear distinction between the “actual” position of $\{ut, 0, 0\}$ of the charged particle at the instant t we are considering, and its retarded position $\mathbf{r}'(t')$, where t' is the solution of Eq. (13), i.e. the moment when the “signal” from the particle reaches the observation point \mathbf{r} .

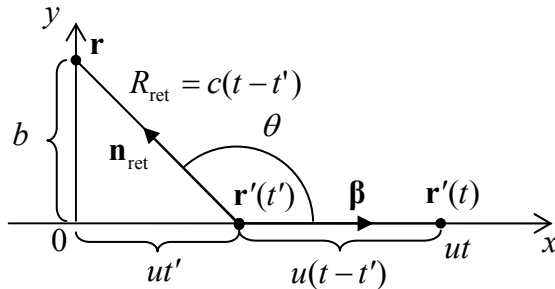


Fig. 10.3. Geometry of the linearly moving charge problem.

⁵ Superficially, this may seem to contradict to electrostatics where \mathbf{B} should vanish while \mathbf{E} stay finite. However, note that according to the Coulomb law for a point charge, in this case $\mathbf{E} = E\mathbf{n} = E\mathbf{n}_{\text{ret}}$, so that $\mathbf{B} \propto \mathbf{n}_{\text{ret}} \times \mathbf{E} = 0$.

In these coordinates

$$\boldsymbol{\beta} = \{\beta, 0, 0\}, \quad \mathbf{r} = \{0, 0, b\}, \quad \mathbf{r}'_{\text{ret}} = \{ut', 0, 0\}, \quad \mathbf{n}_{\text{ret}} = \{\cos\theta, 0, \sin\theta\}, \quad (10.21)$$

with $\cos\theta = -ut'/R_{\text{ret}}$, so that $[(\mathbf{n} - \boldsymbol{\beta})_x]_{\text{ret}} = -ut'/R_{\text{ret}} - \beta$, and for the longitudinal component of the electric field, Eq. (20a) yields

$$E_x = \frac{q}{4\pi\epsilon_0} \left[\frac{-ut'/R - \beta}{\gamma^2(1 - \boldsymbol{\beta} \cdot \mathbf{n})^3 R^2} \right]_{\text{ret}} = \frac{q}{4\pi\epsilon_0} \left[\frac{-ut' - \beta R}{\gamma^2(1 - \boldsymbol{\beta} \cdot \mathbf{n})^3 R^3} \right]_{\text{ret}}. \quad (10.22)$$

But according to Eq. (13), product βR_{ret} may be presented as $\beta c(t - t') = u(t - t')$. Plugging this expression into Eq. (22), we are eliminating the explicit dependence of E_x on time t' :

$$E_x = \frac{q}{4\pi\epsilon_0} \frac{-ut}{\gamma^2 [(1 - \boldsymbol{\beta} \cdot \mathbf{n})R]_{\text{ret}}^3}. \quad (10.23)$$

The transversal components of the field also have a similar form:

$$E_y = \frac{q}{4\pi\epsilon_0} \left[\frac{\sin\theta}{\gamma^2(1 - \boldsymbol{\beta} \cdot \mathbf{n})^3 R^2} \right]_{\text{ret}} = \frac{q}{4\pi\epsilon_0} \frac{b}{\gamma^2 [(1 - \boldsymbol{\beta} \cdot \mathbf{n})R]_{\text{ret}}^3}, \quad E_z = 0. \quad (10.24)$$

Hence, the only combination of t' and R_{ret} we still need to calculate is $[(1 - \boldsymbol{\beta} \cdot \mathbf{n})R]_{\text{ret}}$. From Fig. 3, $\boldsymbol{\beta} \cdot \mathbf{n}_{\text{ret}} = \beta \cos\theta = -\beta ut'/R_{\text{ret}}$, so that $(1 - \boldsymbol{\beta} \cdot \mathbf{n})R_{\text{ret}} = R_{\text{ret}} + \beta ut' = c(t - t') + c\beta^2 t' = ct - ct'/\gamma^2$. What remains is to find time t' from the self-consistency equation (4) which in our case (Fig. 3) takes the form

$$R_{\text{ret}}^2 \equiv c^2(t - t')^2 = b^2 + (ut')^2. \quad (10.25)$$

After solving this quadratic equation (with the appropriate negative sign before the square root, in order to get $t' < t$),

$$t' = \gamma^2 t - \left[(\gamma^2 t)^2 - \gamma^2 (t^2 - b^2/c^2) \right]^{1/2} = \gamma^2 t - \frac{\gamma}{c} (u^2 \gamma^2 t^2 + b^2)^{1/2}, \quad (10.26)$$

we obtain a simple result:

$$[(1 - \boldsymbol{\beta} \cdot \mathbf{n})R]_{\text{ret}} = \frac{c}{\gamma^2} (u^2 \gamma^2 t^2 + b^2)^{1/2}, \quad (10.27)$$

so that the electric field components are

$$E_x = -\frac{q}{4\pi\epsilon_0} \frac{\gamma ut}{(b^2 + \gamma^2 u^2 t^2)^{3/2}}, \quad E_y = \frac{q}{4\pi\epsilon_0} \frac{\gamma b}{(b^2 + \gamma^2 u^2 t^2)^{3/2}}, \quad E_z = 0. \quad (10.28)$$

These are exactly Eqs. (9.139) which had been obtained in Sec. 9.5 by simpler means, without the necessity to solve the self-consistency equation for t' .⁶ However, that alternative approach was essentially based on the inertial motion of the particle, and cannot be used in problems in which particle moves with acceleration. In those problems, the second term in Eq. (20a), describing EM wave radiation, is essential and most important.

⁶ A similar calculation of magnetic field components from Eq. (20b) gives the results identical to Eqs. (9.140).

10.2. Radiation

Let us calculate the angular distribution of particle's radiation. For that, we need to return to use Eqs. (20) to find the Poynting vector $\mathbf{S} = \mathbf{E} \times \mathbf{H}$, and in particular its component $S_n = \mathbf{S} \cdot \mathbf{n}_{\text{ret}}$, at large distance R from the particle. Following tradition, let us express the result as the radiated energy per unit solid angle per unit time interval dt' of the *radiation* (rather than its *measurement*), using Eq. (18):

$$\frac{d\mathcal{P}}{d\Omega} \equiv -\frac{d\mathcal{E}}{d\Omega dt'} = \left[R^2 S_n \frac{dt}{dt'} \right]_{\text{ret}} = R_{\text{ret}}^2 (\mathbf{E} \times \mathbf{H}) \cdot \mathbf{n}_{\text{ret}} (1 - \boldsymbol{\beta} \cdot \mathbf{n})_{\text{ret}}. \quad (10.29)$$

At sufficiently large distances from the particle, i.e. in the limit $R \rightarrow \infty$,⁷ the contribution of the first (essentially, the Coulomb interaction) term in the square brackets of Eq. (20a) vanishes as $1/R^2$, so that we get a key formula valid for arbitrary law of particle motion:

$$\frac{d\mathcal{P}}{d\Omega} = \frac{Z_0 q^2}{(4\pi)^2} \frac{|\mathbf{n} \times [(\mathbf{n} - \boldsymbol{\beta}) \times \dot{\boldsymbol{\beta}}]|^2}{(1 - \mathbf{n} \cdot \boldsymbol{\beta})^5}. \quad (10.30)$$

Now, let us apply this important result to some simple cases. First of all, Eq. (30) says that a charge moving with constant velocity $\boldsymbol{\beta}$ does not radiate at all. (This might be expected from our analysis of this case in Sec. 9.5, because in the reference frame moving with the charge it produces only the Coulomb electrostatic field, i.e. evidently no radiation.)

Next, let us consider a linear motion of a point charge, but with finite acceleration – evidently directed along the same straight line, like it takes place in linear accelerators. With the coordinate axes directed as shown in Fig. 4a, each of the vectors involved in Eq. (30) has at most two nonvanishing Cartesian components:

$$\mathbf{n} = \{\sin \theta, 0, \cos \theta\}, \quad \boldsymbol{\beta} = \{0, 0, \beta\}, \quad \dot{\boldsymbol{\beta}} = \{0, 0, \dot{\beta}\}. \quad (10.31)$$

where θ is the angle between the directions of particle's motion and radiation propagation.

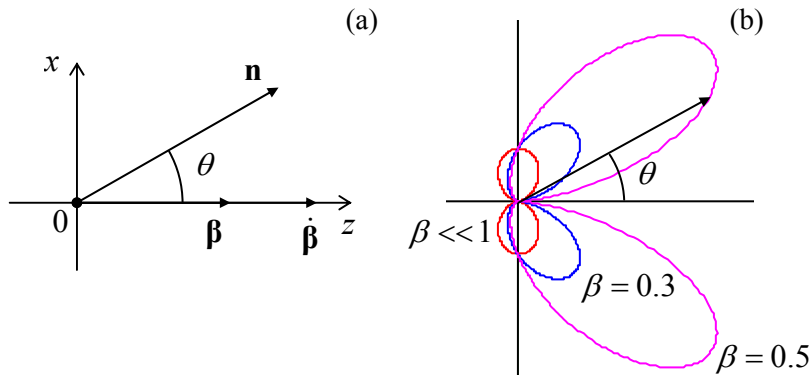


Fig. 10.4. Radiation at linear acceleration: (a) geometry of the problem, and (b) the last fraction in Eq. (32) as a function of angle θ .

Plugging these expressions into Eq. (30) and performing the vector multiplications, we get

$$\frac{d\mathcal{P}}{d\Omega} = \frac{Z_0 q^2}{(4\pi)^2} \dot{\beta}^2 \frac{\sin^2 \theta}{(1 - \beta \cos \theta)^5}. \quad (10.32)$$

⁷ In this limit, the distinction between points \mathbf{r}' and \mathbf{r} is evident (for example, vector \mathbf{n} does not depend on particle's position), and we may drop index "ret".

Figure 4b shows the angular distribution of this radiation, for three values of particle speed. If particle's velocity is relatively low ($\beta \ll 1$), the denominator in Eq. (32) is close to 1 for all θ , so that the angular distribution of the radiation power is close to $\sin^2\theta$ - just as required by the general nonrelativistic formula (8.26). However, as the velocity is increased, the denominator is less than 1 for $\theta < \pi/2$, i.e. for the forward-looking directions, and is larger than 1 for back directions. As a result, the radiation toward particle's velocity is increased (regardless of the acceleration sign!), while that in the back direction is suppressed. For ultrarelativistic particles ($\beta \rightarrow 1$), this trend is enormously exacerbated, and radiation to small forward angles dominates. In order to describe this main part of the distribution, we may expand the trigonometric functions of θ , participating in Eq. (32), into the Taylor series in small θ , and keep only their leading terms: $\sin\theta \approx \theta$, $\cos\theta \approx 1 - \theta^2/2$, so that $(1 - \beta\cos\theta) \approx (1 + \gamma^2\theta^2)/2\gamma^2$. The resulting expression,

$$\frac{d\mathcal{P}}{d\Omega} \approx \frac{2Z_0q^2}{\pi^2} \dot{\beta}^2 \gamma^8 \frac{(\gamma\theta)^2}{(1 + \gamma^2\theta^2)^5}, \quad (10.33)$$

describes a peak of radiation with a maximum at

$$\theta_0 \approx \frac{1}{2\gamma} \ll 1. \quad (10.34)$$

Note that due to the axial symmetry of the result, and the fact that $d\mathcal{P}/d\Omega = 0$ in the exact direction of particle's propagation ($\theta = 0$), Eq. (40) describes a narrow circular "hollow cone" of radiation. Another important aspect of this result is how fast does the maximum radiation brightness grow with the Lorentz factor γ , i.e. with particle's energy $\mathcal{E} = \gamma mc^2$. Still, the total radiated power \mathcal{P} at linear acceleration is not too high for any practicable values of parameters.

In order to show this, let us first calculate \mathcal{P} for an arbitrary motion of the particle. It is possible to do this by a straightforward integration of Eq. (30) over the full solid angle, but let me demonstrate how \mathcal{P} may be found (or rather guessed) from general relativistic arguments. In Sec. 8.2, we have derived Eq. (8.27) for the electric dipole radiation for nonrelativistic particle motion. That result is valid, in particular, of one charged particle whose electric dipole moment's derivative over time may be expressed as $d(q\mathbf{r})/dt = (q/m)\mathbf{p}$, where \mathbf{p} is particle's mechanical momentum. As the result, Eq. (8.27) (in free space, i.e. with $v = c$) reduces to

$$\mathcal{P} = \frac{Z_0}{6\pi c^2} \left(\frac{q}{m} \frac{d\mathbf{p}}{dt} \right)^2 = \frac{Z_0 q^2}{6\pi m^2 c^2} \left(\frac{d\mathbf{p}}{dt} \cdot \frac{d\mathbf{p}}{dt} \right). \quad (10.35)$$

This is evidently not a Lorentz-invariant result, but it gives a clear hint how such an invariant,⁸ which would be identical to Eq. (35) in the nonrelativistic limit, may be formed:

$$\mathcal{P} = -\frac{Z_0 q^2}{6\pi m^2 c^2} \left(\frac{dp_\alpha}{d\tau} \cdot \frac{dp^\alpha}{d\tau} \right) = \frac{Z_0 q^2}{6\pi m^2 c^2} \left[\left(\frac{d\mathbf{p}}{d\tau} \right)^2 - \frac{1}{c^2} \left(\frac{d\mathcal{E}}{d\tau} \right)^2 \right]. \quad (10.36)$$

⁸ Strictly speaking, I would need to prove the (almost evident) fact that \mathcal{P} is indeed Lorentz-invariant, but I will not go into this, because all the "derivation" of Eq. (36) is not much more than an illustration of the heuristic power of the 4-vector formalism.

Plugging in the relativistic expressions, $\mathbf{p} = \gamma mc\boldsymbol{\beta}$, $\mathcal{E} = \gamma mc^2$, and $d\tau = dt/\gamma$, the last formula may be recast in the form

$$\mathcal{P} = \frac{Z_0 q^2}{6\pi} \gamma^6 \left[(\dot{\boldsymbol{\beta}})^2 - (\boldsymbol{\beta} \times \dot{\boldsymbol{\beta}})^2 \right], \quad (10.37)$$

which may be also obtained by a direct integration of Eq. (30), thus confirming our guess. However, for most applications, it is beneficial to express \mathcal{P} the via the time evolution of particle's momentum alone. For that, we may differentiate the fundamental relativistic relation (9.78), $\mathcal{E}^2 = (mc^2)^2 + (pc)^2$, over the proper time τ to get

$$2\mathcal{E} \frac{d\mathcal{E}}{d\tau} = 2c^2 p \frac{dp}{d\tau}, \quad \text{i.e.} \quad \frac{d\mathcal{E}}{d\tau} = \frac{c^2 p}{\mathcal{E}} \frac{dp}{d\tau} = u \frac{dp}{d\tau}, \quad (10.38)$$

where, at the last transition, the magnitude of the relativistic vector relation $c^2 \mathbf{p}/\mathcal{E} = \mathbf{u}$ has been used. Plugging this relation into Eq. (36), we may rewrite it as

$$\mathcal{P} = \frac{Z_0 q^2}{6\pi m^2 c^2} \left[\left(\frac{d\mathbf{p}}{d\tau} \right)^2 - \beta^2 \left(\frac{dp}{d\tau} \right)^2 \right]. \quad (10.39)$$

Note the difference between the squared derivatives: in the first of them we differentiate the momentum vector \mathbf{p} , and only then form a scalar by squaring it, while in the second case, the magnitude of the vector is differentiated to start with. For example, for a circular motion with constant speed (to be analyzed in the next section), the second term is zero, while the first is not. However, if we return to the simplest case of linear acceleration (Fig. 4), then $(d\mathbf{p}/d\tau)^2 = (dp/d\tau)^2$, and Eq. (39) is reduced to

$$\mathcal{P} = \frac{Z_0 q^2}{6\pi m^2 c^2} \left(\frac{dp}{d\tau} \right)^2 (1 - \beta^2) = \frac{Z_0 q^2}{6\pi m^2 c^2} \left(\frac{dp}{d\tau} \right)^2 \frac{1}{\gamma^2} = \frac{Z_0 q^2}{6\pi m^2 c^2} \left(\frac{dp}{dt'} \right)^2, \quad (10.40)$$

i.e. formally coincides with nonrelativistic Eq. (35).

In order to get a better feeling of the magnitude of this radiation, we may use the fact that $dp/dt = d\mathcal{E}/dz'$. This allows us to rewrite Eq. (40) in the following form:

$$\mathcal{P} = \frac{Z_0 q^2}{6\pi m^2 c^2} \left(\frac{d\mathcal{E}}{dz} \right)^2 = \frac{Z_0 q^2}{6\pi m^2 c^2} \frac{d\mathcal{E}}{dz'} \frac{d\mathcal{E}}{dt'} \frac{dt'}{dz'} = \frac{Z_0 q^2}{6\pi m^2 c^2 u} \frac{d\mathcal{E}}{dz'} \frac{d\mathcal{E}}{dt'}. \quad (10.41)$$

For the most important case of ultrarelativistic motion ($u \rightarrow c$), this result may be presented as

$$\frac{\mathcal{P}}{d\mathcal{E}/dt'} \approx \frac{2}{3} \frac{d(\mathcal{E}/mc^2)}{d(z'/r_c)}, \quad (10.42)$$

where r_c is the classical radius of the particle, given by Eq. (8.41). This formula shows that the radiated power, i.e. the change of particle's energy due to radiation, is much smaller than that due to the accelerating field, unless energy as large as mc^2 is gained on the classical radius of the particle. For example, for an electron, such acceleration would require the accelerating electric field of the order of $(0.5 \text{ MV})/(3 \times 10^{-15} \text{ m}) \sim 10^{14} \text{ MV/m}$, while the practical accelerating fields are below 10^3 MV/m , limited by the electric breakdown effects. In the next section, we will see that in circular accelerators, the radiation is much larger. Such smallness of EM radiative losses is actually a large advantage of linear

electron accelerators - such as the famous 2-mile-long SLAC (<http://www.slac.stanford.edu/>) which can accelerate electrons or positrons to energies up to 50 GeV ($\gamma \sim 10^5$).

10.3. Synchrotron radiation

Consider now a charged particle being accelerated in the direction perpendicular to its velocity \mathbf{u} (for example by the magnetic component of the Lorentz force), so that its speed u , and hence the magnitude p of its momentum, do not change. In this case, the second term in Eq. (39) vanishes, and it yields

$$\mathcal{P} = \frac{Z_0 q^2}{6\pi m^2 c^2} \left(\frac{d\mathbf{p}}{d\tau} \right)^2 = \frac{Z_0 q^2}{6\pi m^2 c^2} \left(\frac{d\mathbf{p}}{dt'} \right)^2 \gamma^2. \quad (10.43)$$

Comparing this expression with Eq. (40), we see that for the same acceleration magnitude, the EM radiation is a factor of γ^2 larger. For modern accelerators, with $\gamma \sim 10^4$ - 10^5 , such a factor creates a huge difference!

For example, if the particle is on a cyclotron orbit in a constant magnetic field (as was analyzed in Sec. 9.6), both \mathbf{u} and $\mathbf{p} = \gamma m \mathbf{u}$ obey Eq. (9.150), so that

$$\left| \frac{d\mathbf{p}}{dt'} \right| = \omega_c p = \frac{u}{R} p = \beta^2 \gamma \frac{mc^2}{R}, \quad (10.44)$$

so that for the power of this *synchrotron radiation*, Eq. (43) yields

$$\mathcal{P} = \frac{Z_0 q^2}{6\pi} \beta^4 \gamma^4 \frac{c^2}{R^2}. \quad (10.45)$$

According to Eq. (9.153), at fixed magnetic field (in particle accelerators, limited to a few Tesla produced by the beam-bending magnets), the synchrotron orbit radius R scales as γ , so that according to Eq. (45), \mathcal{P} scales as γ^2 , i.e. grows fast with particle's energy $\mathcal{E} \propto \gamma$. For example, for typical parameters of first electron cyclotrons (such as the General Electric synchrotron in which the synchrotron radiation was first noticed in 1947), $R \sim 1$ m, $\mathcal{E} \sim 0.3$ GeV ($\gamma \sim 600$), Eq. (45) gives the electron energy loss per one revolution, $\mathcal{P}\Delta t' \approx 2\pi\mathcal{P}R/c \sim 1$ keV. However, already by the mid-1970s, electron accelerators, with $R \sim 100$ m, have reached energies $\mathcal{E} \sim 10$ GeV, and the energy loss per revolution has grown to ~ 10 MeV, becoming the major energy loss mechanism.⁹ However, what is bad for accelerators and storage rings is good for the so-called *synchrotron light sources*: electron accelerators designed exactly for the generation of intensive synchrotron radiation - with the spectrum well beyond the visible light range. Let us now analyze the angular and spectral distributions of such radiation.

To calculate the angular distribution, let us select the coordinate axes as shown in Fig. 5, with the origin at the current location of the orbiting particle, axis z along its instant velocity (i.e. vector $\boldsymbol{\beta}$),

⁹ For proton accelerators, such energy loss is much less of a problem, because γ of an ultrarelativistic particle (at fixed \mathcal{E}) is proportional to $1/m$, so that the estimates, at the same R , should be scaled back by $(m_p/m_e)^4 \sim 10^{13}$. Nevertheless, in the giant modern accelerators such as the LHC (with $R \approx 4.3$ km and $\mathcal{E} \approx 7$ TeV), the synchrotron radiation loss per revolution is rather noticeable ($\mathcal{P}\Delta t' \sim 6$ keV), leading not as much to particle deceleration as to substantial photoelectron emission from the beam tube walls, creating harmful defocusing effects.

and axis x toward the orbit center. In the general case, the unit vector \mathbf{n} toward the radiation observer is not in any of the coordinate planes, and hence should be described by two angles – the polar angle θ and the azimuthal angle φ between the x axis and projection OP of vector \mathbf{n} on plane $[x, y]$. Since the length of segment OP is $\sin\theta$, the Cartesian coordinates of the relevant vectors are as follows:

$$\mathbf{n} = \{\sin\theta \cos\varphi, \sin\theta \sin\varphi, \cos\theta\}, \quad \boldsymbol{\beta} = \{0, 0, \beta\}, \quad \dot{\boldsymbol{\beta}} = \{\dot{\beta}, 0, 0\}. \quad (10.46)$$

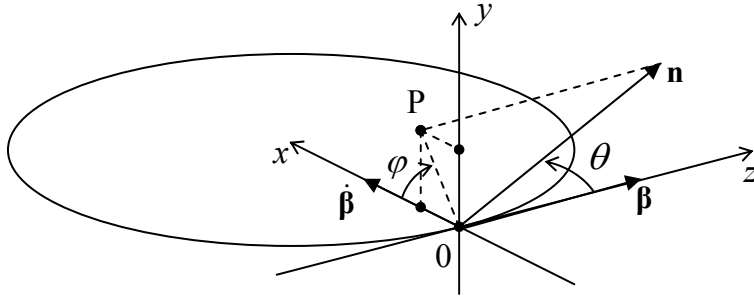


Fig. 10.5. Geometry of the synchrotron radiation problem.

Plugging these coordinates into the general Eq. (30), we get

$$\frac{d\mathcal{P}}{d\Omega} = \frac{2Z_0q^2}{\pi^2} |\dot{\boldsymbol{\beta}}|^2 \gamma^6 f(\theta, \varphi), \quad f(\theta, \varphi) \equiv \frac{1}{8\gamma^6 (1 - \beta \cos\theta)^3} \left[1 - \frac{\sin^2\theta \cos^2\varphi}{\gamma^2 (1 - \beta \cos\theta)^2} \right], \quad (10.47)$$

Just as at the linear acceleration, in the most important ultrarelativistic limit, most radiation goes to a narrow cone (of width $\Delta\theta \sim \gamma^{-1} \ll 1$) around vector $\boldsymbol{\beta}$, i.e. along the instant direction of particle's propagation. For such small angles, and $\gamma \gg 1$, the second of Eqs. (47) is reduced to

$$f(\theta, \varphi) \approx \frac{1}{(1 + \gamma^2 \theta^2)^3} \left[1 - \frac{4\gamma^2 \theta^2 \cos^2\varphi}{(1 + \gamma^2 \theta^2)^2} \right]. \quad (10.48)$$

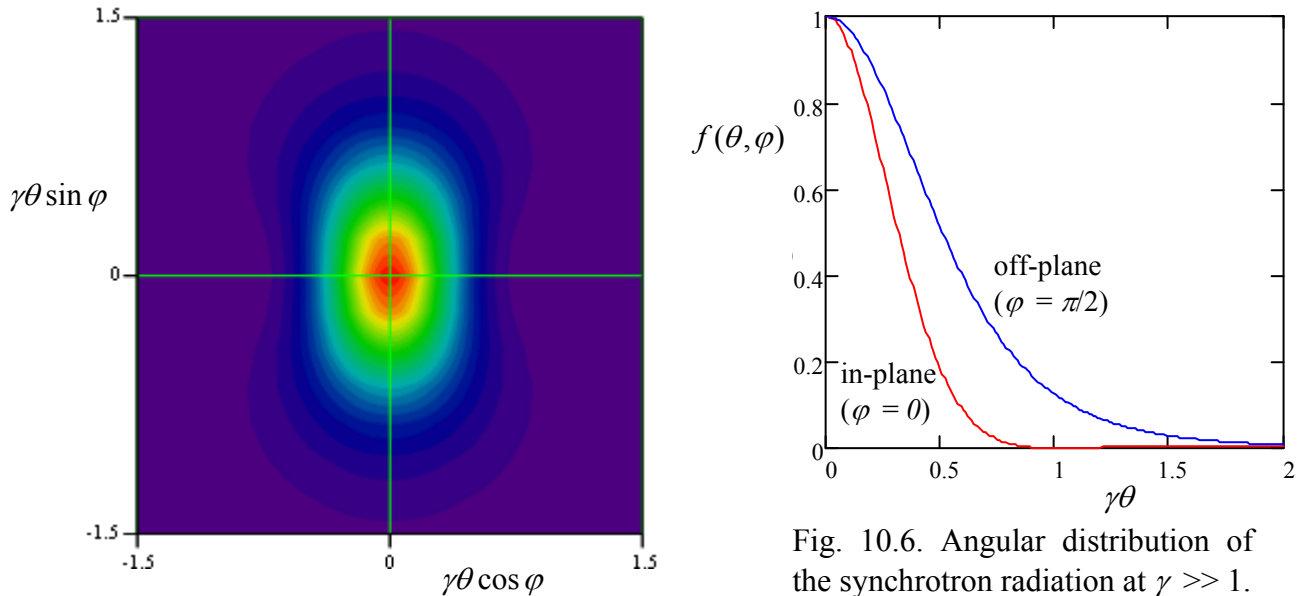


Fig. 10.6. Angular distribution of the synchrotron radiation at $\gamma \gg 1$.

The left panel of Fig. 6 shows the angular distribution $f(\theta, \varphi)$ color-coded, in the plane perpendicular to particle's instant velocity (in Fig. 5, plane $[x, y]$), while its right panel shows the intensity as a function of θ in two perpendicular directions: within the particle rotation plane (axis x) and perpendicular to this plane (axis y). The result shows, first of all, that, in contrast to the case of linear acceleration, the narrow radiation cone is now not hollow: the intensity maximum is reached exactly at $\theta = 0$, i.e. in particle's instant direction. Second, the radiation cone is not axially-symmetric: the intensity drops faster within the particle rotation plane (and even has nodes at $\theta = \pm 1/\gamma$).

Now let us consider the time/frequency structure of the synchrotron radiation, now from the point of view of the observer rather than the particle itself. (In the latter picture, due to the axial symmetry of the problem, the total radiation power \mathcal{P} is evidently constant.) Its semi-quantitative picture may be obtained from the angular distribution we have just analyzed. Indeed, if an ultrarelativistic particle's radiation is observed from a point in (or close to) the rotation plane,¹⁰ the observer is being “struck” by the narrow radiation cone once each rotation period, each “strike” giving a pulse of a short duration $\Delta t \ll \omega_c$ – see Fig. 7.

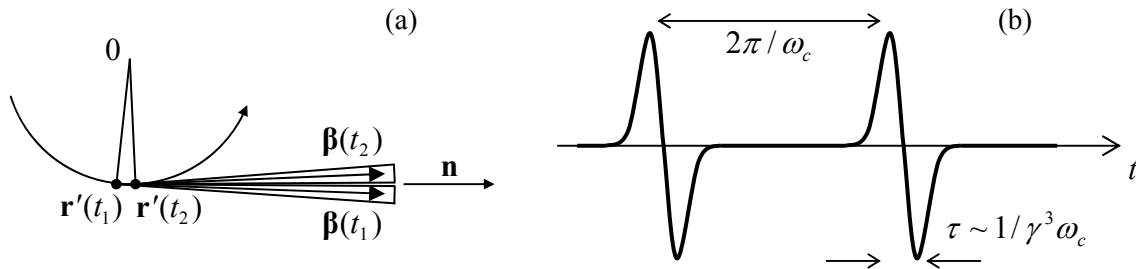


Fig. 10.7. (a) Synchrotron radiation “cones” at $\gamma \gg 1$, and (b) the in-plane component of their electric field observed in the rotation plane – schematically.

The estimate of the time duration Δt of each pulse, however, requires care: its naïve estimate, $\sim 1/\gamma\omega_c$, would be wrong. Indeed, such estimate, $\Delta t' \sim 1/\gamma\omega_c$ is correct for the duration of the time of particle's motion while its cone is aimed at the observer. However, due to the time compression effect, discussed in detail in Sec. 1 and described by Eqs. (12) and (18), the pulse duration as seen by observer is a factor of $1/(1 - \beta)$ shorter, so that

$$\tau = (1 - \beta)\tau' \sim \frac{1 - \beta}{\gamma\omega_c} \sim \frac{1}{\gamma^3\omega_c}. \quad (10.49)$$

Applying the Fourier theorem to this pattern, we can expect that the frequency spectrum of the radiation consists of numerous ($N \sim \gamma^3 \gg 1$) harmonics of the rotation frequency ω_c , with comparable amplitudes. However, if the orbital frequency fluctuates even slightly ($\delta\omega_c/\omega_c > 1/N \sim 1/\gamma^3$), as it happens in most practical systems, the radiation pulses are not coherent, so that the average radiation spectrum may be calculated as that of one pulse, multiplied by number of pulses per second. In this case, the spectrum is continuous, extending from low frequencies all the way to approximately

$$\omega_{\max} \sim 1/\tau \sim \gamma^3\omega_c. \quad (10.50)$$

¹⁰ If the observation point is off-plane, or if the rotation speed is much less than c , the radiation is virtually monochromatic, with frequency ω_c .

In order to verify this estimate, let us calculate the spectrum of radiation, due to a single pulse. For that, we should first make the general notion of spectrum quantitative. Let us present an arbitrary electric field (say that of the radiation we are studying now), considered as a function of the observation time t (at fixed \mathbf{r}), as a Fourier integral:¹¹

$$\mathbf{E}(t) = \int_{-\infty}^{+\infty} \mathbf{E}_\omega e^{-i\omega t} dt. \quad (10.51)$$

Let us plug this into the expression for total energy of the EM pulse (i.e. of particle energy's loss) per unit solid angle,¹²

$$-\frac{d\mathcal{E}}{d\Omega} \equiv \int_{-\infty}^{+\infty} S_n(t) R^2 dt = \frac{R^2}{Z_0} \int_{-\infty}^{+\infty} |\mathbf{E}(t)|^2 dt. \quad (10.52)$$

This substitution, plus a natural change of integration order, yield

$$\frac{d\mathcal{E}}{d\Omega} = \frac{R^2}{Z_0} \int_{-\omega}^{+\omega} d\omega \int_{-\omega}^{+\omega} d\omega' \mathbf{E}_\omega \cdot \mathbf{E}_{\omega'} \int_{-\infty}^{+\infty} dt e^{-i(\omega+\omega')t}. \quad (10.53)$$

But the inner integral (over t) is just $2\pi\delta(\omega + \omega')$.¹³ This delta-function kills one of the frequency integrals (say, one over ω'), and Eq. (54) gives the result which may be recast as

$$-\frac{d\mathcal{E}}{d\Omega} = \int_0^{+\infty} I(\omega) d\omega, \quad I(\omega) = \frac{4\pi R^2}{Z_0} \mathbf{E}_\omega \cdot \mathbf{E}_{-\omega} = 4\pi Z_0 \varepsilon_0^2 (cR)^2 \mathbf{E}_\omega \mathbf{E}_\omega^*, \quad (10.54)$$

where the evident frequency symmetry of the scalar product $\mathbf{E}_\omega \cdot \mathbf{E}_{-\omega}$ has been utilized to fold the integral of $I(\omega)$ to positive frequencies only. The first of Eqs. (51) and the first of Eqs. (54) make the physical sense of function $I(\omega)$ crystal-clear: this is the so-called *spectral density* of EM radiation (per unit solid angle per unit pulse).¹⁴

In order to calculate the density, we need to express function \mathbf{E}_ω via $\mathbf{E}(t)$ using the reciprocal Fourier theorem:

$$\mathbf{E}_\omega = \frac{1}{2\pi} \int_{-\infty}^{+\omega} \mathbf{E}(t) e^{i\omega t} dt. \quad (10.55)$$

In the particular case of radiation by a single point charge, we should use the second term of Eq. (20a):

$$\mathbf{E}_\omega = \frac{1}{2\pi} \frac{q}{4\pi\varepsilon_0} \frac{1}{cR} \int_{-\infty}^{+\infty} \frac{\mathbf{n} \times \{(\mathbf{n} - \boldsymbol{\beta}) \times \dot{\boldsymbol{\beta}}\}}{(1 - \boldsymbol{\beta} \cdot \mathbf{n})^3} e^{i\omega t} dt. \quad (10.56)$$

¹¹ In contrast to the single-frequency case (i.e. a monochromatic wave), we may avoid taking real part of the complex function ($\mathbf{E}_\omega e^{-i\omega t}$) if we require that $\mathbf{E}_{-\omega} = \mathbf{E}_\omega^*$. However, it is important to remember the factor $1/2$ required for the transition to a monochromatic wave of frequency ω_0 : $\mathbf{E}_\omega = \mathbf{E}_0 [\delta(\omega - \omega_0) + \delta(\omega + \omega_0)]/2$.

¹² Note that the expression under the integral differs from $d\mathcal{P}/d\Omega$ defined by Eq. (29) by the absence of term $(1 - \boldsymbol{\beta} \cdot \mathbf{n}) = \partial t' / \partial t$. This is natural, because this is the wave energy arriving to the observation point \mathbf{r} in time interval dt (rather than dt').

¹³ See, e.g. MA Eq. (14.3a).

¹⁴ The notion of spectral density may be readily generalized to random processes – see, e.g., SM Sec. 5.4.

Since vectors \mathbf{n} and $\boldsymbol{\beta}$ are typically known as functions of the radiation (retarded) time t' , let us use Eqs. (18) to change integration in Eq. (52) from the observation time t to time t' :

$$\mathbf{E}_\omega = \frac{q}{4\pi\epsilon_0} \frac{1}{2\pi} \frac{1}{cR} \int_{-\infty}^{+\infty} \frac{\mathbf{n} \times \{(\mathbf{n} - \boldsymbol{\beta}) \times \dot{\boldsymbol{\beta}}\}}{(1 - \boldsymbol{\beta} \cdot \mathbf{n})^2} \exp\left\{i\omega\left(t' + \frac{R_{\text{ret}}}{c}\right)\right\} dt'. \quad (10.57)$$

The strong inequality $R \gg r'$ which we implied from the beginning of this section allows us to consider the unit vector \mathbf{n} as constant and, moreover, to use approximation (8.19) to reduce Eq. (57) to

$$\mathbf{E}_\omega = \frac{1}{2\pi} \frac{q}{4\pi\epsilon_0} \frac{1}{cR} \exp\left\{\frac{i\omega r}{c}\right\} \int_{-\infty}^{+\infty} \frac{\mathbf{n} \times \{(\mathbf{n} - \boldsymbol{\beta}) \times \dot{\boldsymbol{\beta}}\}}{(1 - \boldsymbol{\beta} \cdot \mathbf{n})^2} \exp\left\{i\omega\left(t' - \frac{\mathbf{n} \cdot \mathbf{r}'}{c}\right)\right\} dt', \quad (10.58)$$

Plugging this expression into Eq. (54), we get¹⁵

$$I(\omega) = \frac{Z_0 q^2}{16\pi^3} \left| \int_{-\infty}^{+\infty} \frac{\mathbf{n} \times \{(\mathbf{n} - \boldsymbol{\beta}) \times \dot{\boldsymbol{\beta}}\}}{(1 - \boldsymbol{\beta} \cdot \mathbf{n})^2} \exp\left\{i\omega\left(t' - \frac{\mathbf{n} \cdot \mathbf{r}'}{c}\right)\right\} dt' \right|^2. \quad (10.59)$$

Let me remind the reader that $\boldsymbol{\beta}$ inside this integral is supposed to be taken at the retarded point $\{\mathbf{r}', t'\}$, so that Eq. (58) is fully sufficient for finding the spectral density from the law $\mathbf{r}'(t')$ of particle's motion. However, this result may be further simplified by noticing that the fraction before the exponent may be presented as a full derivative over t' ,

$$\frac{\mathbf{n} \times \{(\mathbf{n} - \boldsymbol{\beta}) \times d\boldsymbol{\beta}/dt'\}}{(1 - \boldsymbol{\beta} \cdot \mathbf{n})^2} = \frac{d}{dt'} \left[\frac{\mathbf{n} \times (\mathbf{n} \times \boldsymbol{\beta})}{1 - \boldsymbol{\beta} \cdot \mathbf{n}} \right], \quad (10.60)$$

and working out the resulting integral by parts. At this operation, time differentiation of the parentheses in the exponent, $d(t' - \mathbf{n} \cdot \mathbf{r}'/c)/dt' = 1 - \mathbf{n} \cdot \mathbf{u}/c = 1 - \boldsymbol{\beta} \cdot \mathbf{n}$, leads to the cancellation of the denominator remains and hence to a surprisingly simple result:¹⁶

$$I(\omega) = \frac{Z_0 q^2 \omega^2}{16\pi^3} \left| \int_{-\infty}^{+\infty} \mathbf{n} \times (\mathbf{n} \times \boldsymbol{\beta}) \exp\left\{i\omega\left(t' - \frac{\mathbf{n} \cdot \mathbf{r}'}{c}\right)\right\} dt' \right|^2. \quad (10.61)$$

Returning to the particular case of synchrotron radiation, it is beneficial to choose the origin of time t' so that at $t' = 0$, angle θ takes its smallest value θ_0 , i.e., in terms of Fig. 5, vector \mathbf{n} is within plane $[y, z]$. Fixing this direction of axes in time, we can redraw that figure as shown in Fig. 7. In these coordinates,

$$\mathbf{n} = \{0, \sin \theta_0, \cos \theta_0\}, \quad \mathbf{r}' = \{R(1 - \cos \alpha), 0, R \sin \alpha\}, \quad \boldsymbol{\beta} \equiv \{\beta \sin \alpha, 0, \beta \cos \alpha\}, \quad (10.62)$$

where $\alpha \equiv \omega c t'$, and an easy multiplication yields

¹⁵ Note that for our current purposes of calculation of spectral density of radiation by a single particle, factor $\exp\{i\omega r/c\}$ has got cancelled. However, as we have seen in Chapter 8, this factor plays the central role at interference of radiation from several (many) sources. In the context of synchrotron radiation, such interference becomes important in *undulators* and *free-electron lasers* - the devices to be (qualitatively) discussed below.

¹⁶ Actually, this simplification is not occasional. According to Eq. (10b), the expression under the derivative is just the transversal component of the vector-potential \mathbf{A} (give or take a constant factor), and from the discussion in Sec. 8.2 we know that this component determines the electric dipole radiation of the particle (which dominates in our current case of uncompensated electric charge).

$$\mathbf{n} \times (\mathbf{n} \times \boldsymbol{\beta}) = \beta \left\{ \sin \alpha, \sin \theta_0 \cos \theta_0 \cos \alpha, -\sin^2 \theta_0 \sin \alpha \right\}, \quad (10.63)$$

$$\exp \left\{ i\omega \left(t' - \frac{\mathbf{n} \cdot \mathbf{r}'}{c} \right) \right\} = \exp \left\{ i\omega \left(t' - \frac{R}{c} \cos \theta_0 \sin \alpha \right) \right\}. \quad (10.64)$$

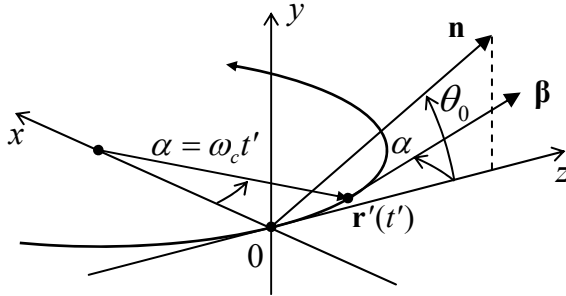


Fig. 10.7. Deriving the spectral density of synchrotron radiation. Vector \mathbf{n} is fixed in plane $[y, z]$, while vectors $\mathbf{r}'(t')$ and $\boldsymbol{\beta}(t')$ rotate in plane $[x, y]$ with angular velocity ω_c .

As we already know, in the (most interesting) ultrarelativistic limit $\gamma \gg 1$, most radiation is confined to narrow pulses, so that only small $\alpha \sim \omega_c \Delta t' \sim \gamma^{-1}$ should contribute to the integral in Eq. (61). Moreover, since most radiation goes to small angles $\theta \sim \gamma^{-1}$, it makes sense to consider only small angles $\theta_0 \sim \gamma^{-1} \ll 1$. Expanding both trigonometric functions of these small angles, participating in parentheses of Eq. (64), into Taylor series, and keeping only terms up to $O(\gamma^{-3})$, we can present them as

$$\left(t' - \frac{R}{c} \cos \theta_0 \sin \alpha \right) = \left(t' - \frac{R}{c} \omega_c t' + \frac{R}{c} \frac{\theta_0^2}{2} \omega_c t' + \frac{R}{c} \frac{\omega_c^3 t'^3}{6} \right). \quad (10.65)$$

Since $(R/c)\omega_c = u/c = \beta \approx 1$, in two last terms we may approximate this parameter by 1. However, it is crucial to distinguish the difference of two first terms, proportional to $(1 - \beta)t'$, from zero, and as we have done before we may approximate it with $t'/2\gamma^2$. In Eq. (63), which does not have such critical differences, we may be more bold, taking¹⁷

$$\mathbf{n} \times (\mathbf{n} \times \boldsymbol{\beta}) \approx \{\alpha, \theta_0, 0\} = \{\omega_c t', \theta_0, 0\}. \quad (10.66)$$

As a result, Eq. (61) is reduced to

$$I(\omega) = \frac{Z_0 q^2}{16\pi^3} |a_x \mathbf{n}_x + a_y \mathbf{n}_y|^2 = \frac{Z_0 q^2}{16\pi^3} (|a_x|^2 + |a_y|^2), \quad (10.67)$$

where the dimensionless factors

$$a_x = \omega \int_{-\infty}^{+\infty} \omega_c t' \exp \left\{ \frac{i\omega}{2} \left((\theta_0^2 + \gamma^{-2})t' + \frac{\omega_c^2}{3} t'^3 \right) \right\} dt', \quad a_y = \omega \int_{-\infty}^{+\infty} \theta_0 \exp \left\{ \frac{i\omega}{2} \left((\theta_0^2 + \gamma^{-2})t' + \frac{\omega_c^2}{3} t'^3 \right) \right\} dt', \quad (10.68)$$

describe the frequency spectra of two components of the synchrotron radiation, with mutually perpendicular directions of polarization. Defining a dimensionless parameter

¹⁷ By the way, this expression shows that the in-plane (x) component of the electric field is an odd function of t' (and hence t – see its sketch in Fig. 7), while the perpendicular component is an even function of time. Also notice that for an observer exactly in the rotation plane ($\theta_0 = 0$) the latter component vanishes.

$$\nu \equiv \frac{\omega}{3\omega_c} (\theta_0^2 + \gamma^{-2})^{3/2}, \quad (10.68)$$

and changing the integration variable to $\xi \equiv \omega_c t' / (\theta_0^2 + \gamma^{-2})^{1/2}$, integrals (67) are reduced to modified Bessel functions of the second kind:

$$a_x = \frac{\omega}{\omega_c} (\theta_0^2 + \gamma^{-2}) \int_{-\infty}^{+\infty} \xi \exp\left\{\frac{3}{2} i \nu \left(\xi + \frac{\xi^3}{3}\right)\right\} d\xi = \frac{2\sqrt{3} i}{(\theta_0^2 + \gamma^{-2})^{1/2}} \nu K_{2/3}(\nu), \quad (10.67a)$$

$$a_y = \frac{\omega}{\omega_c} \theta_0 (\theta_0^2 + \gamma^{-2})^{1/2} \int_{-\infty}^{+\infty} \exp\left\{\frac{3}{2} i \nu \left(\xi + \frac{\xi^3}{3}\right)\right\} d\xi = \frac{2\sqrt{3} \theta_0}{\theta_0^2 + \gamma^{-2}} \nu K_{1/3}(\nu). \quad (10.67b)$$

Figure 8a shows the dependence of amplitudes a_x and a_y of the normalized frequency ν . It is clear that the in-plane component, proportional to a_x , is larger. (The off-plane component disappears altogether at $\theta_0 = 0$, i.e. at observation within the particle rotation plane $[x, y]$, due to the evident mirror symmetry of the problem relative to the plane.) It is also clear that the spectrum changes rather slowly (note the log-log scale of the plot!) until the normalized frequency, defined by Eq. (68) reaches ~ 1 . For most important observation angles $\theta_0 \sim \gamma$ this means that our estimate (50) is indeed correct, though theoretically the frequency spectrum extends to infinity.¹⁸

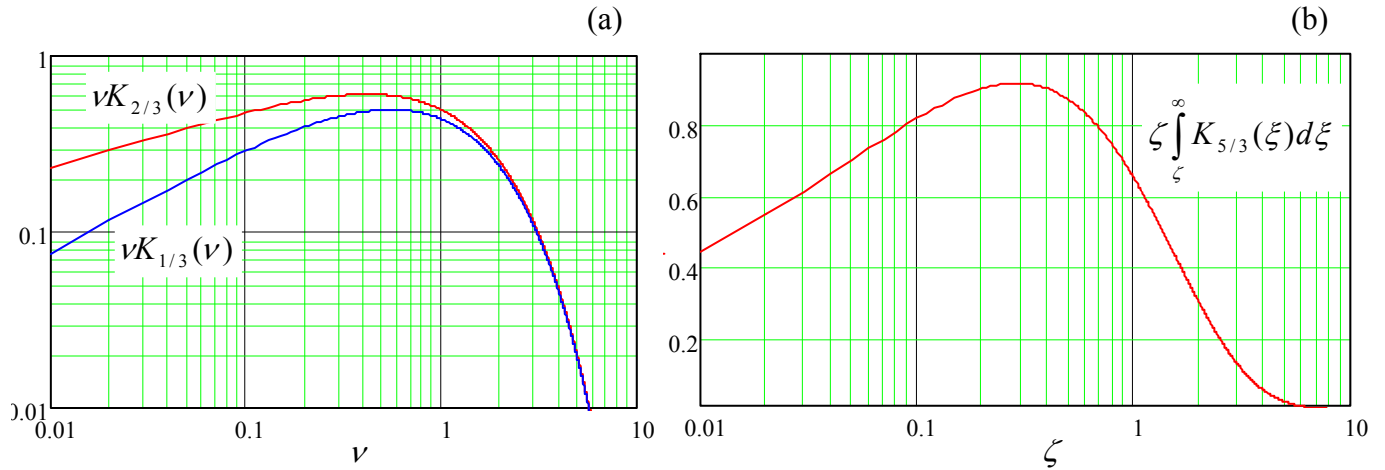


Fig. 10.8. Synchrotron radiation frequency spectra of: (a) two polarization amplitudes and (b) the total (polarization- and angle-averaged) radiation.

Naturally, a similar frequency behavior is valid for the spectral density integrated over the full body angle. Without performing the integration,¹⁹ let me give the result (also valid for $\gamma \gg 1$ only) for reader's reference:

¹⁸ The law of the spectral density decrease at large ν may be readily obtained from the second of Eqs. (2.158) which is valid even for any (even non-integer) index n : $a_x \propto a_y \propto \nu^{1/2} \exp\{-\nu\}$.

¹⁹ See, e.g., the fundamental 5-volume collection E. E. Koch *et al.* (eds.) *Handbook on Synchrotron Radiation* (in 5 vols.), North-Holland, 1983-1991 or a more concise monograph A. Hofmann, *The Physics of Synchrotron Radiation*, Cambridge U. Press, 2007.

$$\oint_{4\pi} I(\omega) d\Omega = \sqrt{3} \frac{q^2}{4\pi} \gamma \zeta \int_{\zeta}^{\infty} K_{5/3}(\xi) d\xi, \quad \zeta \equiv \frac{2}{3} \frac{\omega}{\omega_c \gamma^3}. \quad (10.68)$$

Figure 8b shows the dependence of this integral on normalized frequency ζ . (This plot is sometimes called the “universal flux curve”.) In accordance with estimate (50), it reaches maximum at

$$\zeta_{\max} \approx 0.3, \quad \text{i.e. } \omega_{\max} \approx \frac{\omega_c}{2} \gamma^3. \quad (10.69)$$

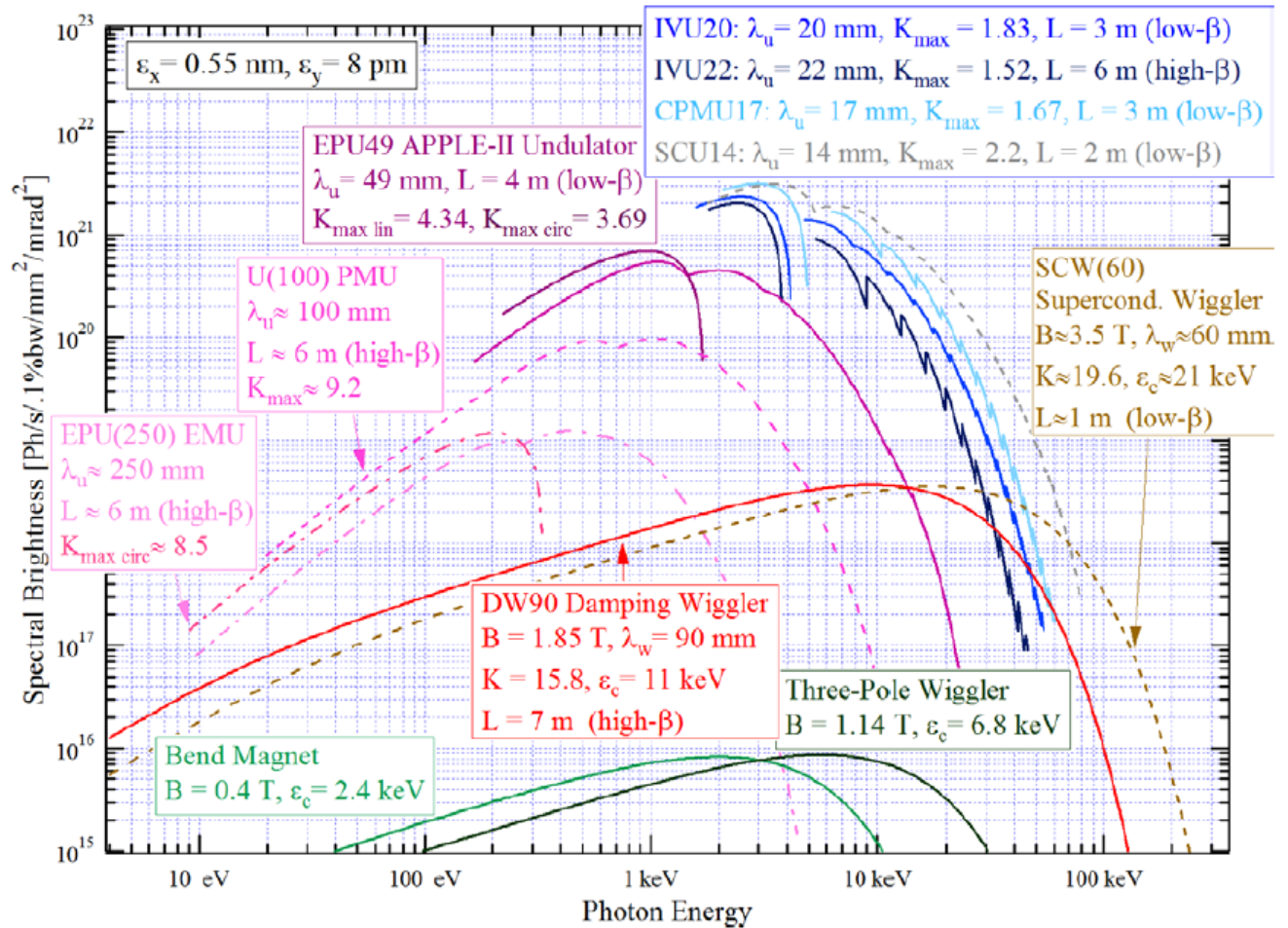


Fig. 10.9. Design brightness of various synchrotron radiation sources of the NSLS-II facility. For bend magnets and wigglers, the “brightness” may be obtained by multiplication of the spectral density $I(\omega)$ from one electron pulse, calculated above, by the number of electrons passing the source per second. (Note the non-SI units, commonly used in the synchrotron radiation community.) However, for undulators, there is an additional factor due to the partial coherence of radiation – see below. (Data from document *NSLS-II Source Properties and Floor Layout*, available online at <http://www.nsls.bnl.gov/>.)

For the new National Synchrotron Light Source (NSLS-II) which is under construction very close to us, in the Brookhaven National Laboratory, with ring circumference of 792 m, the electron revolution period T will be $2.64 \mu\text{s}$. Calculating ω_c as $2\pi/T \approx 2.4 \times 10^6 \text{ s}^{-1}$, for the planned $\gamma \approx 6 \times 10^3$ ($\mathcal{E} \approx$

3 GeV),²⁰ we get $\omega_{\max} \sim 3 \times 10^{17} \text{ s}^{-1}$, corresponding to photon energy $\hbar\omega_{\max} \sim 200 \text{ eV}$ (soft X-rays). In the light of this estimate, the reader may be surprised by Fig. 9 which shows the projected spectra of radiation which this facility is designed to produce.

The reason of this discrepancy is that in NLLS-II, and in all modern synchrotron light sources, most radiation is produced not by the circular orbit itself, but using special devices inserted into the electron beam path. These devices include:

- *bend magnets* with magnetic field stronger than the average field on the orbit, which, according to Eq. (9.112), produce higher effective value of ω_c and hence of ω_{\max} ,
- *wigglers* and *undulators*: strings of several strong magnets with alternating field direction (Fig. 10), which induce periodic bending of electron trajectory, with radiation emitted at each bend.

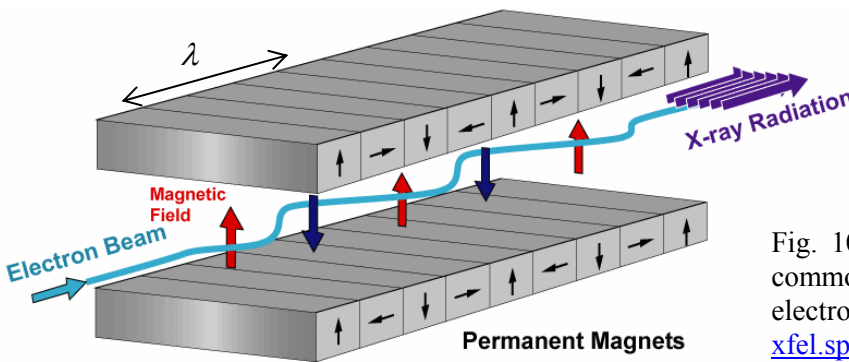


Fig. 10.10. The generic magnetic structure common for wigglers, undulators and free-electron lasers. Adapted from <http://www-xfel.spring8.or.jp/cband/e/Undulator.htm>

The difference between wigglers and undulators is more quantitative than qualitative: the former devices have a larger spatial period λ (distance between the adjacent magnets of the same polarity, see Fig. 10), giving enough space for the magnetic beam to bend by an angle larger than γ^{-1} , i.e. larger than the radiation cone angle. As a result, the pulses radiated at each period arrive to an in-plane observer as a series of individual pulses (Fig. Fig. 11a). The shape of each pulse, and hence its frequency spectrum, are similar to those discussed above,²¹ but with much higher local values of ω_c and ω_{\max} – see Fig. 9. Another difference is a much higher frequency of the peaks. Indeed, the fundamental Eq. (18) allows us to calculate the time distance between them, for the observer, as

$$\Delta t \approx \frac{\partial t}{\partial t'} \Delta t' \approx (1 - \beta) \frac{\lambda}{u} \approx \frac{1}{2\gamma^2} \frac{\lambda}{c} \ll \frac{\lambda}{c}, \quad (10.70)$$

where the first two relations are valid at $\lambda \ll R$ (the relation typically satisfied very well, see Fig. 9), and the last two relations also require the ultrarelativistic limit. As a result, the radiation intensity, which is proportional to the number of poles, is much higher than that from the bend magnets – in the NLSL-II case, more than by 2 orders of magnitude, clearly visible in Fig. 9.

²⁰ By modern standards, this energy is not too high. The distinguished feature of NSLS-II is its unprecedented electron beam intensity (planned average beam current up to 500 mA) which should allow an extremely high synchrotron “brightness” $I(\omega)$.

²¹ A small problem for the reader: use Eq. (66) to explain the difference between shapes of pulses generated at opposite magnetic poles of the wiggler, which is schematically shown in Fig. 11a.

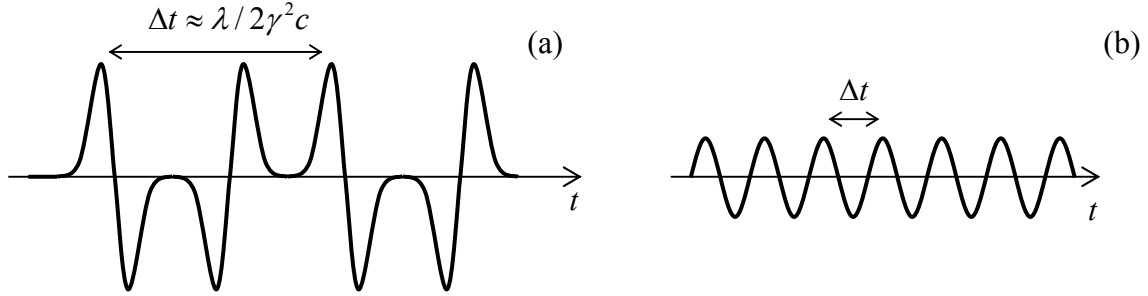


Fig. 10.11. Radiation (with in-plane polarization) from (a) a wiggler and (b) an undulator – schematically.

The situation changes in undulators – similar structures with smaller spatial period λ , in which electron's velocity vector oscillates with angular amplitude smaller than γ^{-1} . As a result, the radiation pulses overlap (Fig. 11b) and the radiation waveform is closer to sinusoidal one. As a result, the radiation spectrum narrows to central frequency²²

$$\omega_0 = \frac{2\pi}{\Delta t} \approx 2\gamma^2 \frac{2\pi c}{\lambda}. \quad (10.70)$$

For example, for the LSNL-II undulators with $\lambda = 20$ mm, this formula predicts the radiation peak at photon energy $\hbar\omega_0 \approx 4$ keV, in a reasonable agreement with results of quantitative calculations, shown in Fig. 9.²³ Due to the spectrum narrowing, the intensity of undulators radiation is higher than that of wigglers using the same electron beam.

This spectrum-narrowing trend is led to its logical conclusion in the so-called *free-electron lasers*²⁴ whose basic structure is the same as that of wigglers and undulators (Fig. 10), but the radiation at each beam bend is so intense and narrow-focused that it affects electron motion downstream the radiation cone. As a result, the radiation of all bends becomes synchronized, so its spectrum is a narrow line at frequency (70), with EM wave amplitude proportional to the number N of electrons in the structure, and hence its power proportional to N^2 (rather than to N as in wigglers and undulators).

Finally, note that wigglers, undulators, and free-electron lasers may be used at the end of linear electron accelerators (such as SLAC) which, as was noted above, may provide extremely high values of γ , and hence radiation frequencies (70), due to the absence of radiation losses at the electron acceleration stage.

²² This important formula may be also interpreted in the following way. Due to the relativistic length contraction (9.20), the undulators period as perceived by beam electrons is $\lambda' = \lambda/\gamma$, so that the central frequency of radiation is $\omega_0' = 2\pi/\lambda' = 2\pi\gamma/\lambda$. For the lab-frame observer, this frequency is Doppler-upshifted according to Eq. (9.44): $\omega_0 = \omega_0' [(1 + \beta)/(1 - \beta)]^{1/2} \approx 2\gamma\omega_0'$, giving the same result (70).

²³ Much of the difference is due to the fact that those plots show the spectral density of the number of *photons* $n = \mathcal{E}/\hbar\omega$ per second, which peaks above the density of power, i.e. energy \mathcal{E} per second.

²⁴ This name is somewhat misleading, because in contrast to the usual (“quantum”) lasers, the free-electron laser operation is essentially classical and very similar to that of vacuum-tube microwave generators (such as magnetrons briefly discussed in Sec. 9.6) – see, e.g., E. L. Salin, E. V. Schneidmiller, and M. V. Yurkov, *The Physics of Free Electron Lasers*, Springer, 2000.

10.4. Bremsstrahlung and Coulomb losses

Surprisingly, a very similar mechanism of radiation by charged particles works at much lower spatial scale – at their scattering by charges of the ordinary (e.g., condensed) matter - the so-called *bremsstrahlung* (German for “brake radiation”).²⁵ This effect responsible, in particular, for the continuous part of the frequency spectrum of the radiation produced by standard vacuum X-ray tubes.

The bremsstrahlung in condensed matter is generally a very complex phenomenon, because at simultaneous involvement of several particles. Also, quantum electrodynamics effects are also frequently important. This is why I will give only a very brief glimpse at the theoretical description of this effect, for the simplest case when scattering of incoming, relatively light charged particles (such as electrons, protons, α -particles, etc.) is produced by atomic nuclei which remain virtually immobile during the scattering event (Fig. 12). This is a reasonable approximation if the energy of incoming particles is not too low, otherwise most scattering is produced by atomic electrons whose dynamics is substantially quantum – see below.

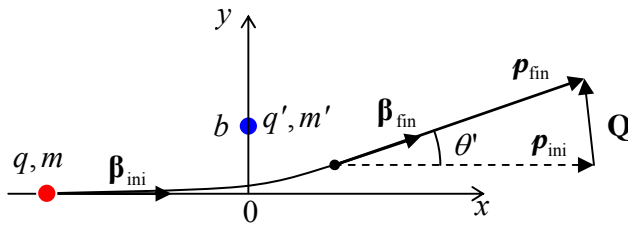


Fig. 10.12. Basic geometry of the bremsstrahlung and Coulomb loss problems.

In order to calculate the frequency spectrum of radiation emitted during a single scattering event, it is convenient to use the byproduct of the last section’s analysis – Eq. (59) with replacement (60):²⁶

$$I(\omega) = \frac{1}{4\pi^2 c} \frac{q^2}{4\pi\epsilon_0} \left| \int_{-\infty}^{+\infty} dt' \left[\frac{\mathbf{n} \times (\mathbf{n} \times \boldsymbol{\beta})}{1 - \boldsymbol{\beta} \cdot \mathbf{n}} \right] \exp \left\{ i\omega \left(t' - \frac{\mathbf{n} \cdot \mathbf{r}'}{c} \right) \right\} dt' \right|^2. \quad (10.71)$$

The typical time τ of a single scattering event, which is described by this formula, is of the order of $a_0/c \sim (10^{-10} \text{ m})/(3 \times 10^8 \text{ m/s}) \sim 10^{-18} \text{ s}$ in solids, and only an order of magnitude longer in gases at ambient conditions. This is why for most frequencies of interest, from zero all the way up to at least soft X-rays,²⁷ we can use the so-called *low-frequency approximation*, taking the exponent in Eq. (71) for 1 through the whole collision event, i.e. the integration interval. This approximation immediately yields

²⁵ The X-ray radiation due to this effect had been observed experimentally (though not correctly interpreted) by Nikola Tesla in 1887, i.e. before the radiation was studied in detail and much publicized by Wilhelm Röntgen.

²⁶ In publications on this topic (whose development peak was in the 1920s and 1930s), Gaussian units are more common, and letter Z is usually reserved for charge multiples in units of the fundamental charge: $q = \pm ze$. This is why, in order to avoid confusion, in this section I will use $1/\epsilon_0 c \equiv Z_0$ for the wave impedance and, still sticking to the same SI units as used through my lecture notes, will write the coefficients in such a form which makes the transfer to the Gaussian units trivial: it is sufficient to replace all $(qq'/4\pi\epsilon_0)_{\text{SI}}$ with $(qq')_{\text{Gaussian}}$.

²⁷ A more careful analysis, taking into account the relativistic factor $(1 - \boldsymbol{\beta} \cdot \mathbf{n})$ which is (as was discussed in the last section) is hidden inside the retarded exponent, shows that this approximation is actually quite reasonable up to much higher frequencies of the order of γ^2/τ .

$$I(\omega) = \frac{1}{4\pi^2 c} \frac{q^2}{4\pi\epsilon_0} \left| \frac{\mathbf{n} \times (\mathbf{n} \times \boldsymbol{\beta}_{\text{fin}})}{1 - \boldsymbol{\beta}_{\text{fin}} \cdot \mathbf{n}} - \frac{\mathbf{n} \times (\mathbf{n} \times \boldsymbol{\beta}_{\text{ini}})}{1 - \boldsymbol{\beta}_{\text{ini}} \cdot \mathbf{n}} \right|^2. \quad (10.72)$$

In the nonrelativistic limit ($\beta_{\text{ini}}, \beta_{\text{fin}} \ll 1$), this expression is reduced to²⁸

$$I(\omega) = \frac{1}{4\pi c} \frac{q^2}{4\pi^2 \epsilon_0} \frac{Q^2}{m^2 c^3} \sin^2 \theta. \quad (10.73)$$

where \mathbf{Q} is the momentum transferred from the scattering center to the scattered charge (Fig. 12):

$$\mathbf{Q} \equiv \mathbf{p}_{\text{fin}} - \mathbf{p}_{\text{ini}} = m\Delta\mathbf{u} = mc\Delta\boldsymbol{\beta} = mc(\boldsymbol{\beta}_{\text{fin}} - \boldsymbol{\beta}_{\text{ini}}), \quad (10.74)$$

and θ is the angle between vector \mathbf{Q} and direction \mathbf{n} toward the observer.

The most important feature of result (73) is the frequency-independent (“white”) spectrum of radiation, very typical for any rapid leaps which may be approximated as theta-functions of time. (Note, however, that this is only valid for a fixed value of Q , so that the statistics of this parameter, to be discussed in a minute, “colors” the radiation.) Note also the angular distribution of the radiation, forming the usual “doughnut” shape about the momentum transfer vector \mathbf{Q} . In particular, this means that in typical cases when $Q \sim p$, the bremsstrahlung produces a significant radiation flow back to the particle source – the fact significant for the operation of X-ray tubes.

Now integrating over all wave propagation angles, just as we did for the instant radiation power in Sec. 8.2, we get the spectral density of their full power,

$$-\frac{d\mathcal{E}}{d\omega} = \oint_{4\pi} I(\omega) d\Omega = \frac{2}{3\pi c} \frac{q^2}{4\pi^2 \epsilon_0} \frac{Q^2}{m^2 c^3}. \quad (10.75)$$

The main new feature of bremsstrahlung, as any scattering problem, is the necessity to use statistics over all possible values of the impact parameter b (Fig. 12) which is unknown for any particular scattering event. For elastic ($\beta_{\text{ini}} = \beta_{\text{fin}} \equiv \beta$) Coulomb collisions we can use the so-called Rutherford formula for the differential cross-section of scattering²⁹

$$\frac{d\sigma}{d\Omega'} = \left(\frac{qq'}{4\pi\epsilon_0} \right)^2 \left(\frac{1}{2pc\beta} \right)^2 \frac{1}{\sin^4(\theta'/2)}. \quad (10.76)$$

Here $d\sigma = 2\pi b db$ is the elementary area of the sample cross-section (as visible from the direction of incident particles) corresponding to particle scattering into an elementary body angle³⁰

$$d\Omega' = 2\pi \sin \theta' |d\theta'|. \quad (10.77)$$

Differentiating the geometric relation which is evident from Fig. 12,

²⁸ Evidently, this result (but not Eq. (72)!) may be derived from Eq. (8.27) as well.

²⁹ See, e.g., CM Eq. (3.72) with appropriate interaction constant $\alpha = qq'/4\pi\epsilon_0$. In the form used in Eq. (76), the formula is also valid for small-angle scattering of relativistic particles, the criterion being $|\Delta\boldsymbol{\beta}| \ll 2/\gamma$.

³⁰ Angle θ' and differential $d\Omega'$, describing the direction of scattered *particles*, should not be confused with θ and $d\Omega$ describing directions of the *radiation* emitted at the scattering event.

$$Q = 2p \sin \frac{\theta'}{2}, \quad (10.78)$$

we may present Eq. (10.76) may be presented in a more convenient form

$$\frac{d\sigma}{dQ} = 8\pi \left(\frac{qq'}{4\pi\epsilon_0} \right)^2 \frac{1}{u^2 Q^3}. \quad (10.79)$$

Now combining Eqs. (75) and (79), we get

$$-\frac{d\mathcal{E}}{d\omega} \frac{d\sigma}{dQ} = \frac{16}{3} \frac{q^2}{4\pi\epsilon_0} \left(\frac{qq'}{4\pi\epsilon_0 mc^2} \right)^2 \frac{1}{c\beta^2} \frac{1}{Q}. \quad (10.80)$$

This product is called the *differential radiation cross-section*. When integrated it over Q (which is equivalent to integration over the impact parameter), it gives a convenient measure of radiation intensity. Indeed, after the multiplication by the volume density n of independent scattering centers, the integral gives particle's energy loss by unit bandwidth of radiation by unit path length, $-d^2\mathcal{E}/d\omega dx$. A technical problem here is that the integral of $1/Q$ formally diverges at both infinite and zero values of Q . However, these divergences are very weak (logarithmic), and the integral converges due to any reason unaccounted for by our simple analysis. The standard simple way to account for these effects is to write

$$-\frac{d^2\mathcal{E}}{d\omega dx} \approx \frac{16}{3} n \frac{q^2}{4\pi\epsilon_0} \left(\frac{qq'}{4\pi\epsilon_0 mc^2} \right)^2 \frac{1}{c\beta^2} \ln \frac{Q_{\max}}{Q_{\min}}, \quad (10.81)$$

and then plug, instead of Q_{\max} and Q_{\min} , scales of the most important effects limiting the small momentum range. At classical analysis, according to Eq. (78), $Q_{\max} = 2p$. To estimate Q_{\min} , let us note that very small momentum transfer takes place when the impact parameter b is very large and hence the effective scattering time $\tau \sim b/v$ is very long. Recalling the condition of the low-frequency approximation, we may associate Q_{\min} with $\tau \sim 1/\omega$ and hence with $b \sim u\tau \sim v/\omega$. Since for the small scattering angles, Q may be estimated as the impulse $F\tau \sim (qq'/4\pi\epsilon_0 b^2)\tau$ of the Coulomb force, so that $Q_{\min} \sim (qq'/4\pi\epsilon_0)\omega/u^2$, and Eq. (81) becomes

$$-\frac{d^2\mathcal{E}}{d\omega dx} \approx \frac{16}{3} n \frac{q^2}{4\pi\epsilon_0} \left(\frac{qq'}{4\pi\epsilon_0 mc^2} \right)^2 \frac{1}{c\beta^2} \ln \left(\frac{4\pi\epsilon_0 2mu^3}{qq'\omega} \right). \quad (10.82)$$

This is *Bohr's formula for classical bremsstrahlung*. We see that the low momentum cutoff indeed makes the spectrum colored, with more energy going to lower frequencies. There is even a formal divergence at $\omega \rightarrow 0$; however, this divergence is integrable, so it does not present a problem in finding the total energy radiative losses ($-d\mathcal{E}/dx$) as an integral of Eq. (82) over all radiated frequencies. A larger problem for this procedure is the upper integration limit, $\omega \rightarrow \infty$, at which the integral diverges. This means that our approximate description, which neglects considers the collision as an elastic process, becomes wrong, and needs to be amended by taking into account the difference $\hbar\omega$ between the initial and final kinetic energies of the particle due to radiation of the energy quantum $\hbar\omega$ of the emitted photon:

$$\frac{p_{\text{ini}}^2}{2m} - \frac{p_{\text{fin}}^2}{2m} = \hbar\omega. \quad (10.83)$$

As a result, taking into account that the minimum and maximum values of Q correspond to, respectively, the parallel and antiparallel alignments of vectors \mathbf{p}_{ini} and \mathbf{p}_{fin} , we get

$$\ln \frac{Q_{\text{max}}}{Q_{\text{min}}} = \ln \frac{p_{\text{ini}} + p_{\text{fin}}}{p_{\text{ini}} - p_{\text{fin}}} = \ln \frac{(p_{\text{ini}} + p_{\text{fin}})^2}{p_{\text{ini}}^2 - p_{\text{fin}}^2} = \ln \frac{[T^{1/2} + (T - \hbar\omega)^{1/2}]^2}{\hbar\omega}. \quad (10.84)$$

Plugged into Eq. (81), this expression yields the so-called *Bethe-Heitler formula for quantum bremsstrahlung*.³¹ Note that at this approach, Q_{max} is close to that of the classical approximation, but $Q_{\text{min}} \sim \hbar\omega/u$, so that

$$\frac{Q_{\text{min}}|_{\text{classical}}}{Q_{\text{min}}|_{\text{quantum}}} \sim \frac{\alpha z z'}{\beta}, \quad (10.85)$$

where z and z' are particles' charges in units of e , and α is the fine structure constant:

$$\alpha \equiv \frac{e^2}{4\pi\epsilon_0\hbar c} \Big|_{\text{SI}} = \frac{e^2}{4\pi\epsilon_0\hbar c} \Big|_{\text{Gaussian}} \approx \frac{1}{137} \ll 1. \quad (10.86)$$

For most cases of practical interest, ratio (85) is smaller than 1, and since we have to keep the highest value of Q_{min} , the Bethe-Heitler formula should be used.

Now nothing prevents us from calculating the total radiative losses of energy per unit length:

$$-\frac{d\mathcal{E}}{dx} = \int_0^{\omega_{\text{max}}} \left(-\frac{d^2\mathcal{E}}{d\omega dz} \right) d\omega = \frac{16}{3} n \frac{q^2}{4\pi\epsilon_0 c} \left(\frac{qq'}{4\pi\epsilon_0 mc^2} \right)^2 \frac{1}{\beta^2} 2 \int_0^{\omega_{\text{max}}} \ln \frac{T^{1/2} - (T - \hbar\omega)^{1/2}}{(\hbar\omega)^{1/2}} d\omega, \quad (10.87)$$

where $\hbar\omega_{\text{max}} = T$ is the maximum energy of the radiation quantum. By introducing the dimensionless integration variable $\xi \equiv \hbar\omega/T = 2\hbar\omega/(mu^2/2)$ this integral is reduced to the table one,³² and we get

$$-\frac{d\mathcal{E}}{dx} = \frac{16}{3} n \frac{q^2}{4\pi\epsilon_0 c} \left(\frac{qq'}{4\pi\epsilon_0 mc^2} \right)^2 \frac{1}{\beta^2} \frac{u^2}{\hbar} = \frac{16}{3} n \left(\frac{q'^2}{4\pi\epsilon_0 \hbar c} \right) \left(\frac{q^2}{4\pi\epsilon_0} \right)^2 \frac{1}{mc^2}. \quad (10.88)$$

In my usual practice, I would give an estimate of the losses for a typical case; however, let me first compare them to a parallel mechanism, the so-called *Coulomb losses*, due to the impulse given by the scattered particle to the scattering center. (This energy eventually goes into the increase of the thermal energy of the scattering matter.) Using Eqs. (9.139) for the electric field of a linearly moving charge, we can readily find the momentum it transfers to charge q' :³³

$$\Delta p' = |(\Delta p')_y| = \left| \int_{-\infty}^{+\infty} (\dot{p}')_y dt \right| = \left| \int_{-\infty}^{+\infty} q'E_y dt \right| = \frac{qq'}{4\pi\epsilon_0} \int_{-\infty}^{+\infty} \frac{\gamma b}{(b^2 + \gamma^2 u^2 t^2)^{3/2}} dt = \frac{qq'}{4\pi\epsilon_0} \frac{2}{bu}. \quad (10.89)$$

³¹ The modifications of this formula necessary for the relativistic case description are surprisingly minor - see, e.g., Chapter 15 of J. D. Jackson, *Classical Electrodynamics*, 3rd ed., Wiley 1999. For more detail, the standard reference monograph on bremsstrahlung is W. Heitler, *The Quantum Theory of Radiation*, 3rd ed., Oxford U. Press 1954 (reprinted in 2010 by Dover).

³² See, e.g., MA Eq. (6.13).

³³ According to Eq. (9.139), $E_z = 0$, and the net impulse of the longitudinal force $q'E_x$ is zero.

Hence, the kinetic energy acquired by the scattering center (i.e. the loss of energy of the incident particle) is

$$-\Delta\mathcal{E} = \frac{(\Delta p')^2}{2m'} = \left(\frac{qq'}{4\pi\epsilon_0} \right)^2 \frac{2}{m'u^2 b^2}. \quad (10.90)$$

Such losses have to be summed up over all collisions, with random values of the impact parameter b . At the charge concentration n per unit volume, the number of collisions per small path length dz per small range db is $dN = n2\pi b db dx$, so that

$$-\frac{d\mathcal{E}}{dx} = \int (-\Delta\mathcal{E}) dN = n \left(\frac{qq'}{4\pi\epsilon_0} \right)^2 \frac{2}{m'u^2} 2\pi \int_{b_{\min}}^{b_{\max}} \frac{db}{b} = 4\pi n \left(\frac{qq'}{4\pi\epsilon_0} \right)^2 \frac{\ln B}{m'u^2}, \quad \text{where } B \equiv \frac{b_{\max}}{b_{\min}}. \quad (10.91)$$

Here the logarithmic integral over b was treated similarly to that over Q in the bremsstrahlung theory. This approach is adequate, because the ratio b_{\max}/b_{\min} is much larger than 1. Indeed, b_{\min} may be estimated from $(\Delta p')_{\max} \sim p = \gamma mu$. For this value, Eq. (89) with $q' \sim q$ gives $b_{\min} \sim r_c$ (see Eq. (8.41) and its discussion), which is, for elementary particles, of the order of 10^{-15} m. On the other hand, for the most important case when charges q' are electrons (which, according to Eq. (91) are the most efficient Coulomb energy absorbers, due to their extremely low mass m'), b_{\max} may be estimated from condition $\tau = b/\gamma u \sim 1/\omega_{\max}$, where $\omega_{\max} \sim 10^{16} \text{ s}^{-1}$ is the characteristic frequency of electron transitions in atoms. (Below this frequency, our classical analysis of scatterer's motion is wrong.) From here, we have the estimate $b_{\max} \sim \gamma u/\omega_{\max}$, so that³⁴

$$B \equiv \frac{b_{\max}}{b_{\min}} \sim \frac{\gamma u}{r_c \omega_0}, \quad (10.92)$$

for $\gamma \sim 1$ and $u \sim c \approx 3 \times 10^8 \text{ m/s}$ giving $b_{\max} \sim 3 \times 10^{-8} \text{ m}$, and $B \sim 10^9$ (give or take a couple orders of magnitude – this does not change the estimate $\ln B \sim 20$ too much).

Now we can compare the Coulomb losses (89) with those due to the bremsstrahlung, given by Eq. (88):

$$\frac{-d\mathcal{E}|_{\text{radiation}}}{-d\mathcal{E}|_{\text{Coulomb}}} \sim \alpha_{zz} \frac{m'}{m} \beta^2 \frac{1}{\ln B}, \quad (10.93)$$

Since $\alpha \sim 10^{-2} \ll 1$, for nonrelativistic particles ($\beta \ll 1$) the Coulomb losses are much higher, and only for ultrarelativistic particles, the relation may be opposite.

³⁴ A quantum analysis (carried out by H. Bethe in 1940) replaces, in Eq. (89), $\ln B$ with

$$\ln \left(\frac{2\gamma^2 m u^2}{\hbar \langle \omega \rangle} \right) - \beta^2,$$

where $\langle \omega \rangle$ is the average frequency of the atomic quantum transitions weight by their oscillator strength. It is clear that this refinement does not change the estimate given below. Note that both the classical and quantum formulas describe, a fast increase (as $1/\beta$) of the energy loss rate ($-d\mathcal{E}/dz$) at $\gamma \rightarrow 1$ and its slow increase (as $\ln \gamma$) at $\gamma \rightarrow \infty$, so that the losses have a minimum at $\gamma - 1 \sim 1$.

According to Eq. (91), for electron-electron scattering ($q = q' = -e$, $m' = m_e$),³⁵ at the value $n = 6 \times 10^{26} \text{ m}^{-3}$ typical for air at ambient conditions, the characteristic length of energy loss,

$$l_c \equiv \frac{T}{(-d\mathcal{E}/dx)}, \quad (10.94)$$

for electrons with kinetic energy $T = 6 \text{ keV}$ is close to $2 \times 10^{-4} \text{ m} = 0.2 \text{ mm}$. (This is why you need vacuum in CRT displays and electron microscope columns!) Since $l_c \propto T^2$, more energetic particles penetrate deeper (until the bremsstrahlung steps in at very high energies)..

10.5. Density effects and the Cherenkov radiation

For condensed matter, the Coulomb loss estimate made in the last section is not quite suitable, because it based on cutoff $b_{\max} \sim \gamma u / \omega_{\max}$. For the example given above, incoming electron velocity u is close to $5 \times 10^7 \text{ m/s}$, and for the typical value $\omega_{\max} \sim 10^{16} \text{ s}^{-1}$ ($\hbar \omega_{\max} \sim 10 \text{ eV}$), this cutoff $b_{\max} \sim 5 \times 10^{-9} \text{ m} = 5 \text{ nm}$. Even for air at ambient conditions, this is larger than the average distance ($\sim 2 \text{ nm}$) between molecules, so that at the high end of the impact parameter range ($b \sim b_{\max}$), the Coulomb loss events in adjacent molecules are not quite independent, and the theory needs corrections. For condensed matter, with much higher particle density n , most collisions satisfy condition

$$nb^3 \gg 1, \quad (10.95)$$

and the treatment of Coulomb collisions as independent events is completely unacceptable. However, condition (95) enables the opposite approach: treating the medium as a continuum. In the time domain approach, used in the previous sections of this chapter, this would be a very complex problem, because it would require an explicit description of medium dynamics. However, the frequency-domain approach, based on the Fourier transform, in both time and space, helps a lot, if functions $\varepsilon(\omega)$ and $\mu(\omega)$ are considered known - either calculated or taken from experiment. Let us have a good look at such approach, because it gives some interesting (and practically important) results.

In Chapter 6, we have used the macroscopic Maxwell equations to derive Eqs. (6.101) which describe the time evolution of potentials in a medium with frequency-independent ε and μ . Looking for all functions in the form of plane-wave expansion³⁶

$$f(\mathbf{r}, t) = \int d^3k \int d\omega f_{\mathbf{k}, \omega} e^{i(\mathbf{k} \cdot \mathbf{r} - \omega t)}, \quad (10.96)$$

and requiring all coefficients at similar exponents to be balanced, we get

$$\left[k^2 - \omega^2 \varepsilon \mu \right] \phi_{\mathbf{k}, \omega} = \frac{\rho_{\mathbf{k}, \omega}}{\varepsilon}, \quad \left[k^2 - \omega^2 \varepsilon \mu \right] \mathbf{A}_{\mathbf{k}, \omega} = \mu \mathbf{j}_{\mathbf{k}, \omega}, \quad (10.97)$$

As was discussed in Chapter 7, in this Fourier form, the Maxwell equations remain valid even for the dispersive media, so that Eq. (97) is generalized as

³⁵ Actually, the above analysis has neglected the change of momentum of the incident particle. This is legitimate at $m' \ll m$, but for $m = m'$ the change approximately doubles the energy losses. Still, this does not change the order of magnitude of the estimate.

³⁶ All integrals here and below are in infinite limits, unless specified otherwise.

$$\left[k^2 - \omega^2 \varepsilon(\omega)\mu(\omega)\right]\phi_{\mathbf{k},\omega} = \frac{\rho_{\mathbf{k},\omega}}{\varepsilon(\omega)}, \quad \left[k^2 - \omega^2 \varepsilon(\omega)\mu(\omega)\right]\mathbf{A}_{\mathbf{k},\omega} = \mu(\omega) \mathbf{j}_{\mathbf{k},\omega}, \quad (10.98)$$

The evident advantage of such equations is that their formal solution is trivial:

$$\phi_{\mathbf{k},\omega} = \frac{\rho_{\mathbf{k},\omega}}{\varepsilon(\omega)\left[k^2 - \omega^2 \varepsilon(\omega)\mu(\omega)\right]}, \quad \mathbf{A}_{\mathbf{k},\omega} = \frac{\mu(\omega) \mathbf{j}_{\mathbf{k},\omega}}{\left[k^2 - \omega^2 \varepsilon(\omega)\mu(\omega)\right]}, \quad (10.99)$$

so that the “only” remaining things to do is to calculate the Fourier transforms of functions $\rho(\mathbf{r}, t)$ and $\mathbf{j}(\mathbf{r}, t)$, using the transform reciprocal to Eq. (96), with one factor $1/2\pi$ per each scalar dimension,

$$f_{\mathbf{k},\omega} = \frac{1}{(2\pi)^4} \int d^3r \int dt f(\mathbf{r}, t) e^{-i(\mathbf{k}\cdot\mathbf{r} - \omega t)}, \quad (10.100)$$

(where all limits are infinite), and then carry out the integration (96).

For our current problem of a single charge q , uniformly moving in the medium with velocity \mathbf{u} ,³⁷

$$\rho(\mathbf{r}, t) = q\delta(\mathbf{r} - \mathbf{u}t), \quad \mathbf{j}(\mathbf{r}, t) = q\mathbf{u}\delta(\mathbf{r} - \mathbf{u}t) = \mathbf{u}\rho(\mathbf{r}, t), \quad (10.101)$$

the first task is easy,

$$\rho_{\mathbf{k},\omega} = \frac{q}{(2\pi)^4} \int d^3r \int dt q\delta(\mathbf{r} - \mathbf{u}t) e^{-i(\mathbf{k}\cdot\mathbf{r} - \omega t)} = \frac{q}{(2\pi)^4} \int e^{i(\omega t - \mathbf{k}\cdot\mathbf{u}t)} dt = \frac{q}{(2\pi)^3} \delta(\omega - \mathbf{k}\cdot\mathbf{u}); \quad (10.102)$$

absolutely similarly,

$$\mathbf{j}_{\mathbf{k},\omega} = \frac{q\mathbf{u}}{(2\pi)^3} \delta(\omega - \mathbf{k}\cdot\mathbf{u}). \quad (10.103)$$

Let us summarize what we have got by now, plugging Eqs. (102) and (103) into Eqs. (99)

$$\phi_{\mathbf{k},\omega} = \frac{1}{(2\pi)^3} \frac{q\delta(\omega - \mathbf{k}\cdot\mathbf{u})}{\varepsilon(\omega)\left[k^2 - \omega^2 \varepsilon(\omega)\mu(\omega)\right]}, \quad \mathbf{A}_{\mathbf{k},\omega} = \frac{1}{(2\pi)^3} \frac{\mu(\omega)q\mathbf{u}\delta(\omega - \mathbf{k}\cdot\mathbf{u})}{\left[k^2 - \omega^2 \varepsilon(\omega)\mu(\omega)\right]} = \varepsilon(\omega)\mu(\omega)\mathbf{u}\phi_{\mathbf{k},\omega}. \quad (10.104)$$

Now, at the last step of calculations, namely integration (96), we are starting to pay heavy price for the easiness of the first steps. This is why let us think well what exactly do we need from it. First of all, for the calculation of power losses, the electric field is more convenient to use than the potentials, so let us calculate the Fourier images of \mathbf{E} and \mathbf{B} . Plugging expansion (96) into relations (6.98), we get

$$\mathbf{E}_{\mathbf{k},\omega} = -i\mathbf{k}\phi_{\mathbf{k},\omega} + i\omega\mathbf{A}_{\mathbf{k},\omega} = i\left[\omega\varepsilon(\omega)\mu(\omega)\mathbf{u} - \mathbf{k}\right]\phi_{\mathbf{k},\omega}, \quad \mathbf{B}_{\mathbf{k},\omega} = i\mathbf{k} \times \mathbf{A}_{\mathbf{k},\omega} = i\varepsilon(\omega)\mu(\omega)\mathbf{k} \times \mathbf{u}\phi_{\mathbf{k},\omega}. \quad (10.105)$$

so that integral (96) is

$$\mathbf{E}(\mathbf{r}, t) = \int d^3k \int d\omega \mathbf{E}_{\mathbf{k},\omega} e^{i(\mathbf{k}\cdot\mathbf{r} - \omega t)} = \frac{iq}{(2\pi)^3} \int d^3k \int d\omega \frac{[\omega\varepsilon(\omega)\mu(\omega)\mathbf{u} - \mathbf{k}]\delta(\omega - \mathbf{k}\cdot\mathbf{u})}{\varepsilon(\omega)\left[k^2 - \omega^2 \varepsilon(\omega)\mu(\omega)\right]} e^{i(\mathbf{k}\cdot\mathbf{r} - \omega t)}. \quad (10.106)$$

³⁷ As was discussed in Sec. 7.2, the Ohmic conductivity σ (generally, also a function of frequency – see, e.g., Eq. (7.44)) may be readily incorporated into the dielectric permittivity: $\varepsilon(\omega) \rightarrow \varepsilon_{\text{ef}}(\omega) + i\sigma(\omega)/\omega$. In this section, I will assume that such incorporation, which is especially natural for the high frequencies, has been performed, so that the current density $\mathbf{j}(\mathbf{r}, t)$ describes only stand-alone currents – in our case, that of the incident particle.

Following Eq. (51), this integral may be partitioned as

$$\mathbf{E}(\mathbf{r}, t) = \int \mathbf{E}_\omega e^{-i\omega t} d\omega, \quad \mathbf{E}_\omega = \int \mathbf{E}_{\mathbf{k}, \omega} e^{i\mathbf{k} \cdot \mathbf{r}} d^3 k = \frac{iq}{(2\pi)^3} \int \frac{[\omega \varepsilon(\omega) \mu(\omega) \mathbf{u} - \mathbf{k}] \delta(\omega - \mathbf{k} \cdot \mathbf{u})}{\varepsilon(\omega) [k^2 - \omega^2 \varepsilon(\omega) \mu(\omega)]} e^{i\mathbf{k} \cdot \mathbf{r}} d^3 k. \quad (10.107)$$

Let us calculate the Cartesian components of the partial Fourier image \mathbf{E}_ω , at a point separated by distance b from particle's trajectory. Selecting the coordinates and time origin as shown in Fig. 9.11a, we have $\mathbf{r} = \{0, b, 0\}$, so that only E_x and E_y are not vanishing.³⁸ In particular, according to Eq. (107),

$$(E_x)_\omega = \frac{iq}{(2\pi)^3 \varepsilon(\omega)} \int dk_x \int dk_y \int dk_z \frac{\omega \varepsilon(\omega) \mu(\omega) u - k_x}{k^2 - \omega^2 \varepsilon(\omega) \mu(\omega)} \delta(\omega - k_x u) e^{ik_y b}. \quad (10.108)$$

The delta-function kills one integral (over k_x) of three, and we get:

$$(E_x)_\omega = \frac{iq}{(2\pi)^3 \varepsilon(\omega) u} \left[\omega \varepsilon(\omega) \mu(\omega) u - \frac{\omega}{u} \right] \int e^{ik_y b} dk_y \int \frac{dk_z}{\omega^2 / u^2 + k_y^2 + k_z^2 - \omega^2 \varepsilon(\omega) \mu(\omega)}. \quad (10.109)$$

The last integral (over k_y) may be readily reduced to the table integral $\int d\xi / (1 + \xi^2)$, in infinite limits, equal to π .³⁹ The result may be presented as

$$(E_x)_\omega = -\frac{i\pi q \kappa^2}{(2\pi)^3 \omega \varepsilon(\omega)} \int \frac{e^{ik_y b}}{(k_y^2 + \kappa^2)^{1/2}} dk_y, \quad (10.110)$$

where parameter κ (generally a complex function of frequency) is defined as

$$\kappa^2 \equiv \omega^2 \left(\frac{1}{u^2} - \varepsilon(\omega) \mu(\omega) \right). \quad (10.111)$$

The last integral may be expressed via the modified Bessel function of the second kind:⁴⁰

$$(E_x)_\omega = -\frac{iqu\kappa^2}{(2\pi)^2 \omega \varepsilon(\omega)} K_0(\kappa b). \quad (10.112)$$

A similar calculation yields

$$(E_y)_\omega = \frac{q\kappa}{(2\pi)^2 \varepsilon(\omega)} K_1(\kappa b). \quad (10.113)$$

Now, instead of rushing to make the final integration (107) over frequency to calculate $\mathbf{E}(t)$, let us realize that what we need for power losses is only the total energy loss through the whole time of particle passage. Energy loss per unit volume is

$$-\frac{d\mathcal{E}}{dV} = \int \mathbf{j} \cdot \mathbf{E} dt, \quad (10.114)$$

³⁸ Note that in comparison with notation of the last section, axes x and z are now swapped.

³⁹ See, e.g., MA Eq. (6.15).

⁴⁰ As a reminder, the main properties of these functions are listed in Sec. 2.5 of these notes – see, in particular, Fig. 2.20 b and Eqs. (157)-(158).

where \mathbf{j} is the current of bound charges in the medium, and should not be confused with the free particle current (101). This integral may be readily expressed via the partial Fourier image \mathbf{E}_ω and the similarly defined image \mathbf{j}_ω , just as it was done at the derivation of Eq. (54):

$$-\frac{d\mathcal{E}}{dV} = \int dt \int d\omega e^{-i\omega t} \int d\omega' e^{-i\omega' t} \mathbf{j}_\omega \cdot \mathbf{E}_{\omega'} = 2\pi \int d\omega \int d\omega' \mathbf{j}_\omega \cdot \mathbf{E}_{\omega'} \delta(\omega + \omega') = 2\pi \int \mathbf{j}_\omega \cdot \mathbf{E}_{-\omega} d\omega. \quad (10.115)$$

In our approach, the Ohmic conductance is incorporated into the complex permittivity $\varepsilon(\omega)$, so that, according to the discussion in the end of Sec. 7.2, current's Fourier image is

$$\mathbf{j}_\omega = \sigma_{\text{ef}}(\omega) \mathbf{E}_\omega = -i\omega \varepsilon(\omega) \mathbf{E}_\omega. \quad (10.116)$$

As a result, Eq. (113) yields

$$-\frac{d\mathcal{E}}{dV} = -2\pi i \int \varepsilon(\omega) \mathbf{E}_\omega \cdot \mathbf{E}_{-\omega} \omega d\omega = 4\pi \text{Im} \int_0^\infty \varepsilon(\omega) |E_\omega|^2 \omega d\omega. \quad (10.117)$$

(The last transition is possible due to the property $\varepsilon(-\omega) = \varepsilon^*(\omega)$ which was discussed in Sec. 7.2.)

Finally, just as in the last section, we have to calculate the energy loss rate averaged over random values of the impact parameter b :

$$-\frac{d\mathcal{E}}{dx} = \int \left(-\frac{d\mathcal{E}}{dV} \right) d^2b = 2\pi \int_{b_{\min}}^\infty \left(-\frac{d\mathcal{E}}{dV} \right) b db = 8\pi^2 \int_{b_{\min}}^\infty b db \int_0^\infty \left(|E_x|_\omega^2 + |E_y|_\omega^2 \right) \text{Im} \varepsilon(\omega) \omega d\omega. \quad (10.118)$$

Note that we are cutting the resulting integral over b from below at some b_{\min} where our theory loses legitimacy. (On that limit, we are not doing anything better than in the previous section). Plugging in the calculated expressions (112) and (113) for field components, swapping the integrals, and using recurrent relations (2.143), which are common for any Bessel functions, we finally get the result:

$$-\frac{d\mathcal{E}}{dx} = \frac{2}{\pi} q^2 \text{Im} \int_0^\infty (\kappa^* b_{\min}) K_1(\kappa^* b_{\min}) K_0(\kappa^* b_{\min}) \frac{d\omega}{\omega \varepsilon(\omega)}. \quad (10.119)$$

This result is valid for an arbitrary linear medium, with arbitrary dispersion relations $\varepsilon(\omega)$ and $\mu(\omega)$. (The last function participates in Eq. (119) via parameter κ - see Eq. (111)). To get more concrete results, we should use some particular model of the medium. Let us use the model of independent harmonic oscillators, which was used in Sec. 7.2 for the discussion of dispersion and attenuation of plane waves, in its modification suitable for transition to quantum-mechanical description of atoms:

$$\varepsilon(\omega) = \varepsilon_0 + \frac{nq'^2}{m} \sum_j \frac{f_j}{(\omega_j^2 - \omega^2) - 2i\omega\delta_j}, \quad \sum_j f_j = 1, \quad \mu(\omega) = \mu_0. \quad (10.120)$$

If the damping of the effective atomic oscillators is low, $\delta_j \ll \omega_j$, and particle's velocity is much lower than the typical EM wave's phase velocity v (and hence $c!$), then for most frequencies

$$\kappa^2 \equiv \omega^2 \left(\frac{1}{u^2} - \frac{1}{v^2(\omega)} \right) \approx \frac{\omega^2}{u^2}, \quad (10.121)$$

i.e. $\kappa = \kappa^* \approx \omega/u$ is real. In this case, Eq. (117) may be shown to give Eq. (91) with

$$b_{\max} = \frac{1.123u}{\langle \omega \rangle}. \quad (10.122)$$

Good news here is that both approaches (the microscopic analysis of Sec. 4 and the macroscopic analysis of this section) give essentially the same result. This fact may be also perceived as bad news: the account of the density effects here did not give any new results. The situation somewhat changes at relativistic velocities at which the density effects may provide noticeable corrections, reducing the energy loss estimates. Another effect is, however, much more important. Indeed, let us consider the dependence of the electric field components on distance b . If $\kappa^2 > 0$, then κ is real, and we can use the asymptotic formula (2.158),

$$K_n(\xi) \rightarrow \left(\frac{\pi}{2\xi} \right)^{1/2} e^{-\xi}, \text{ at } \xi \rightarrow \infty, \quad (10.123)$$

to conclude that the complex amplitudes E_ω of both components E_x and E_y of the electric field decrease exponentially, starting from $b \sim u/\langle \omega \rangle$. However, let us consider what happens at frequencies where $\kappa^2 < 0$, i.e.⁴¹

$$\varepsilon(\omega)\mu(\omega) \equiv \frac{1}{v^2(\omega)} < \frac{1}{u^2} < \frac{1}{c^2} = \varepsilon_0\mu_0. \quad (10.124)$$

(This condition means that particle's velocity is larger than the phase velocity of waves, at this particular frequency.) In these intervals, κ is purely imaginary, functions $\exp\{\kappa b\}$ become just phase factors, and

$$|E_x(\omega)| \propto |E_y(\omega)| \propto \frac{1}{b^{1/2}}. \quad (10.125)$$

This means that the Poynting vector drops as $1/b$, so that its flux through a surface of a round cylinder of radius b , with the axis on the particle trajectory (i.e. power flow), does not depend on b . Hence, this is EM wave radiation – the famous *Cherenkov radiation*.⁴²

The direction of its propagation may be readily found taking into account that at large distances from particle's trajectory the emitted wave has to be locally plane, so that the *Cherenkov angle* θ may be found from the ratio of the field components (Fig. 13a):

$$\tan \theta = -\frac{E_x}{E_y}. \quad (10.126)$$

This ratio may be calculated by plugging the asymptotic formula (123) into Eqs. (112) and (113) and taking their ratio:

$$\tan \theta = -\frac{E_x}{E_y} = \frac{i\kappa u}{\omega} = [\varepsilon(\omega)\mu(\omega)u^2 - 1]^{1/2} = \left(\frac{u^2}{v^2(\omega)} - 1 \right)^{1/2}, \text{ i.e. } \cos \theta = \frac{v(\omega)}{u} < 1. \quad (10.127)$$

⁴¹ Strictly speaking, this inequality does not have sense for a medium with complex $\varepsilon(\omega)\mu(\omega)$, but in a typical medium where particles can propagate, the imaginary part of the product only in very narrow frequency intervals, much more narrow than the intervals which we are now discussing.

⁴² It was observed experimentally by P. Cherenkov (in older Western texts, “Čerenkov”) in 1934 and explained (by I. Frank and E. Tamm) in 1937.

Remarkably, this direction does not depend on the emission instant t' , so that radiation of frequency ω , at each instant, forms a hollow cone led by the particle. This simple result allows an evident interpretation (Fig. 13b): the cone is just the set of all observation points which may be reached by “signals” propagating with speed $v(\omega) < u$ from all previous points of particle’s trajectory.

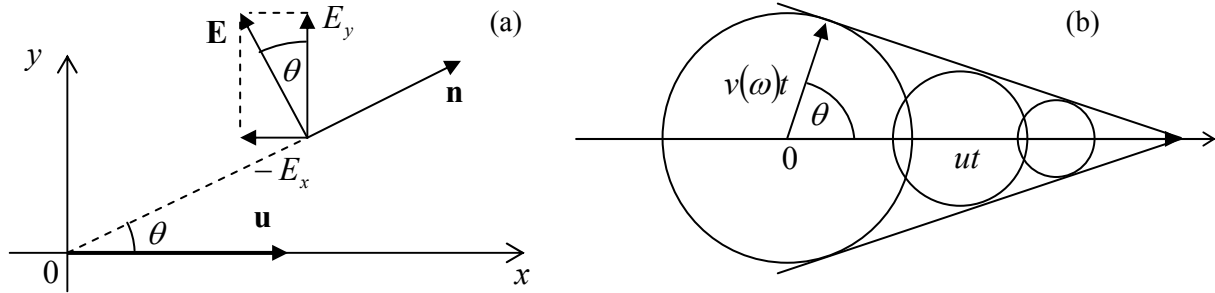


Fig. 10.13. (a) The Cherenkov radiation propagation angle θ , and (b) its interpretation.

This phenomenon is closely related to shock waves, and especially to the so-called *Mach cone*, in fluid dynamics, besides that in the Cherenkov radiation there is a separate cone for each frequency (of the range in which $v(\omega) < u$): the smaller is the $\varepsilon(\omega)\mu(\omega)$ product, i.e. the larger is wave velocity $v(\omega) = 1/[\varepsilon(\omega)\mu(\omega)]^{1/2}$, and the broader is the cone, i.e. the earlier the corresponding “shock wave” arrives to an observer. Please note that the Cherenkov radiation is a unique radiative phenomenon: it takes place even if a particle moves without acceleration, and (in agreement with our analysis in Sec. 2, is impossible in free space where $v = c$ is always larger than u).

The intensity of the Cherenkov radiation intensity may be also readily found by plugging the asymptotic expressions (119), with imaginary κ , into Eq. (119). The result is

$$-\frac{d\mathcal{E}}{dx} \approx \left(\frac{ze}{4\pi}\right)^2 \int_{v(\omega) < u} \omega \left(1 - \frac{u^2}{\varepsilon(\omega)\mu(\omega)}\right) d\omega. \quad (10.128)$$

For nonrelativistic particles ($u \ll c$), the Cherenkov radiation condition $u > v(\omega)$ may be fulfilled only in narrow frequency intervals where the product $\varepsilon(\omega)\mu(\omega)$ is very large (usually, due to optical resonance peaks of the electric permittivity – see Fig. 7.5 and its discussion). In this case the emitted light is nearly monochromatic. On the contrary, if the condition $u > v(\omega)$, i.e. $u^2/\varepsilon(\omega)\mu(\omega) > 1$ is fulfilled in a broad frequency range (as it is for ultrarelativistic particles in condensed media), the radiated power is clearly dominated by higher frequency of the range – hence the bluish color of the Cherenkov radiation glow from water nuclear reactors– see Fig. 14.

The Cherenkov radiation is broadly used for the detection of radiation in high energy experiments for particle identification and speed measurement (since it is easy to pass particles through media of various density and hence of the dielectric constant) – for example, in the so-called Ring Imaging Cherenkov (RICH) detectors which have been designed for the DELPHI experiment⁴³ at the Large Electron-Positron Collider (LEP) in CERN.

⁴³ See, e.g., <http://delphiwww.cern.ch/offline/physics/delphi-detector.html>. For a broader view at radiation detectors (including Cherenkov), the reader may be referred to the classical text by G. F. Knoll, *Radiation*

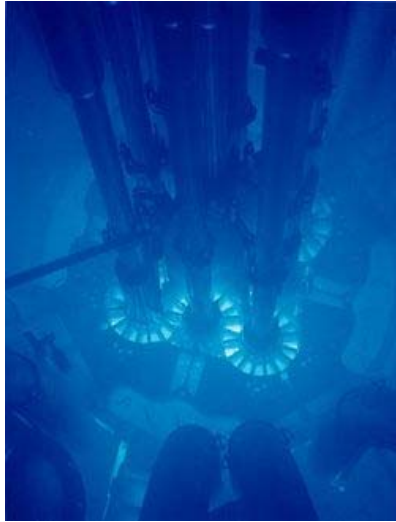


Fig. 10.14. The Cherenkov radiation glow coming from the Advanced Test Reactor of the Idaho National Laboratory. From http://en.wikipedia.org/wiki/Cherenkov_radiation.

A little bit counter-intuitively, the formalism described in this section is very useful for the description of an apparently rather different effect - the so-called *transition radiation* which takes place when a charged particle crosses a border between two media.⁴⁴ The effect may be understood as result of the time dependence of the electric dipole formed by the moving charge and its mirror image in the counterpart medium – see Fig. 16. In the nonrelativistic limit, the effect allows a straightforward description combining the electrostatics picture of Sec. 3.4 (see Fig. 3.9 and its discussion), and Eq. (8.27) slightly corrected for polarization effects of the media. However, if particle's velocity u is comparable with the phase velocity of waves in either medium, the adequate theory of the transition radiation becomes very close to that of the Cherenkov radiation.

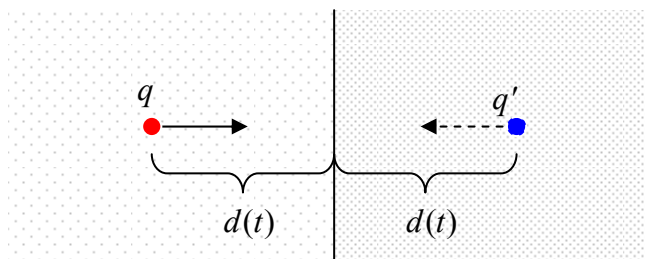


Fig. 10.16. Physics of the transition radiation.

In comparison with the Cherenkov radiation, the transition radiation is rather weak, and its practical use (mostly for the measurement of the relativistic factor γ , to which the radiation intensity is proportional) requires multi-layered stacks.⁴⁵ In these systems, the radiation emitted at sequential borders may be coherent, and the system's physics becomes close to that of undulators.

Detection and Measurement, 4th ed., Wiley, 2010, and a newer treatment by K. Kleinknecht, *Detectors for Particle Radiation*, Cambridge U. Press, 1999.

⁴⁴ The effect was predicted theoretically in 1946 by V. Ginzburg and I. Frank, and only then observed experimentally.

⁴⁵ See, e.g., Sec. 5.3 in K. Kleinknecht's monograph cited above.

10.6. Radiation's back-action

An attentive reader could notice that so far our treatment of charged particle dynamics was never fully self-consistent. Indeed, in Sec. 9.6 we have analyzed particle's motion in various external fields, ignoring the fields radiated by particle itself, while in Sec. 8.2 and earlier in this chapter we have calculated these fields (for several simple cases), but, again, ignored their back-action on the particle. Only in few cases, we have taken the back effects of the radiation implicitly, via the energy conservation. However, even in these cases, the near-field components of the fields, which affect the moving particle most (such as the first term in Eq. (20a)), have been ignored.

At the same time, it is clear that generally the interaction of a point charge with its own field cannot be ignored. As the simplest example, if electron is made to fly through a resonant cavity, thus inducing oscillations in it, and then is forced to return to it before the oscillations decay, its motion will be certainly affected by the oscillating fields, just as if they had been induced by another source. (Fields do not carry any "birth mark".) There is no conceptual problem with the Maxwell theory application to such "field-particle rendezvous" effects; moreover, it is the basis of engineering design of such electron devices as klystrons, magnetrons, and undulators.

The problem arises when no finite "rendezvous" point is enforced by boundary conditions, so that the most important self-field effects are at $R \rightarrow 0$, the most evident example being the radiation of particle in free space, described earlier in this chapter. We already know that radiation takes away a part of charge's kinetic energy, i.e. has to cause its deceleration. One should wonder, however, whether such self-action effects might be described in a more direct, non-perturbative way.

As the first attempt, let us try a phenomenological approach based on the already derived formulas for radiation power \mathcal{P} . For the sake of simplicity, let us consider a nonrelativistic point charge q in free space, so that \mathcal{P} is described by Eq. (8.27), with electric dipole moment's derivative over time equal to $q\mathbf{u}$:

$$\mathcal{P} = \frac{Z_0 q^2}{6\pi c^2} \dot{u}^2 = \frac{2}{3c^3} \frac{q^2}{4\pi\epsilon_0} \dot{u}^2. \quad (10.129)$$

The most naïve approach would be to write the equation of particle's motion in the form

$$m\dot{\mathbf{u}} = \mathbf{F}_{\text{ext}} + \mathbf{F}_{\text{self}}, \quad (10.130)$$

and try to calculate the radiation back-action force by requiring its instant power, $-\mathbf{F}_{\text{self}} \cdot \mathbf{u}$, to be equal to \mathcal{P} . However, this approach (say, for 1D motion) would give a very unnatural result,

$$F_{\text{selfd}} \propto \frac{\dot{u}^2}{u}, \quad (10.131)$$

which may diverge at some points of particle's trajectory. This failure is clearly due to the retardation effect: as we know Eq. (129) results from the analysis of radiation fields at large distances from the particle, e.g., from the second term in Eq. (20a), i.e. when non-radiative first term (which is much larger at $R \rightarrow 0$) is ignored.

Before pursuing term, let us, however, make one more try with Eq. (129), considering its *average* effect on some periodic motion of the particle. To calculate the average, let us write

$$\overline{\dot{\mathbf{u}}^2} \equiv \frac{1}{T} \int_0^T \dot{\mathbf{u}} \cdot \dot{\mathbf{u}} dt, \quad (10.132)$$

and integrate this identity, over the motion period by parts:

$$\overline{\mathcal{P}} = \frac{2}{3c^3} \frac{q^2}{4\pi\epsilon_0} \overline{(\dot{\mathbf{u}})^2} = \frac{2}{3c^3} \frac{q^2}{4\pi\epsilon_0} \frac{1}{T} \left(\dot{\mathbf{u}} \cdot \mathbf{u} \Big|_0^T - \int_0^T \ddot{\mathbf{u}} \cdot \mathbf{u} dt \right) = -\frac{1}{T} \int_0^T \frac{2}{3c^3} \frac{q^2}{4\pi\epsilon_0} \ddot{\mathbf{u}} \cdot \mathbf{u} dt. \quad (10.133)$$

On the other hand, the back-action force would give

$$\overline{\mathcal{P}} = -\frac{1}{T} \int_0^T \mathbf{F}_{\text{rad}} \cdot \mathbf{u} dt. \quad (10.134)$$

These two averages coincide if⁴⁶

$$\mathbf{F}_{\text{self}} = \frac{2}{3c^3} \frac{q^2}{4\pi\epsilon_0} \ddot{\mathbf{u}}. \quad (10.135)$$

This is the so-called *Abraham-Lorentz force* for self-action. Before going after a more serious derivation of this formula, let us estimate its scale, presenting Eq. (135) as

$$\mathbf{F}_{\text{self}} = m \tau \ddot{\mathbf{u}}, \quad \tau \equiv \frac{2}{3mc^3} \frac{q^2}{4\pi\epsilon_0}, \quad (10.136)$$

where constant τ evidently has the dimension of time. Recalling definition (8.41) of the classical radius r_c of the particle, we can present τ as

$$\tau = \frac{2}{3} \frac{r_c}{c}. \quad (10.137)$$

For an electron, τ is of the order of 10^{-23} s. This means that in most cases the Abrahams-Lorentz force is either negligible or leads to the same results as the perturbative treatments of energy loss we have used earlier in this chapter.

However, Eq. (136) brings unpleasant surprises. For example, let us consider a 1D oscillator of eigenfrequency ω_0 . For it, Eq. (130), with the back-action force given by Eq. (136), is

$$m\ddot{x} + m\omega_0^2 x = m\tau \ddot{x}. \quad (10.138)$$

Looking for the solution to this linear differential equation in the usual exponential form, $x(t) \propto \exp\{\lambda t\}$, we get the following characteristic equation,

$$\lambda^2 + \omega_0^2 = \tau \lambda^3. \quad (10.139)$$

⁴⁶ This formula may be readily generalized to the relativistic case:

$$F_{\text{self}}^\alpha = \frac{2}{3mc^3} \frac{q^2}{4\pi\epsilon_0} \left[\frac{d^2 p^\alpha}{d\tau^2} + \frac{p^\alpha}{(mc)^2} \left(\frac{dp_\beta}{d\tau} \frac{dp^\beta}{d\tau} \right) \right],$$

(the so-called *Abraham-Lorentz-Dirac force*).

It may look like that for any “reasonable” value of $\omega_0 \ll 1/\tau \sim 10^{23} \text{ s}^{-1}$, the right-hand side of this nonlinear algebraic equation may be treated as a perturbation. Indeed, looking for its solutions in the natural form $\lambda_{\pm} = \pm i\omega_0 + \lambda'$, with $|\lambda'| \ll \omega_0$, expanding both parts of Eq. (139) in the Taylor series in small parameter λ' , and keeping only linear terms, we get

$$\lambda' \approx -\frac{\omega_0^2 \tau}{2}. \quad (10.140)$$

This means that the energy of free oscillations decreases in time as $\exp\{2\lambda't\} = \exp\{-\omega_0^2 \tau t\}$; this is exactly the radiative damping analyzed earlier. However, Eq. (139) is deceiving; it has the third root corresponding to unphysical, exponentially growing (so-called *run-away*) solutions. It is easiest to see for the free particle, with $\omega_0 = 0$. Then Eq. (139) becomes very simple,

$$\lambda^2 = \tau\lambda^3, \quad (10.141)$$

and it is easy to find all its 3 roots explicitly: $\lambda_1 = \lambda_2 = 0$ and $\lambda_3 = 1/\tau$. While the first 2 roots correspond the values λ_{\pm} found earlier, the last one describes exponential (and extremely fast!) acceleration..

In order to reduce this artifact, let us try to develop a self-consistent approach to back action, taking into account near-field terms of particle fields. For that, we need somehow overcome the divergence of Eqs. (10) and (20) at $R \rightarrow 0$. The most reasonable way is to spread particle charge over a ball of radius scale a , with a spherically-symmetric (but not necessarily constant) density $\rho(r)$, and in the end of calculations trace the limit $a \rightarrow 0$.⁴⁷ Again sticking to the non-relativistic case (so that the magnetic component of the Lorentz force is not important), we should calculate

$$\mathbf{F}_{\text{rad}} = \int_V \rho(\mathbf{r}) \mathbf{E}(\mathbf{r}, t) d^3 r, \quad (10.142)$$

where the electric field is that of the particle itself, with field of any elementary charge $dq = \rho(r)d^3 r$, described by Eqs. (20a).

In order to make analytical calculations doable, we need to make assumption $a \ll r_c$, treat ratio $R/r_c \sim a/r_c$ as a small parameter, and expand the result in the Taylor series in R . This procedure yields

$$\mathbf{F}_{\text{self}} = -\frac{2}{3} \frac{1}{4\pi\epsilon_0} \sum_{n=0}^{\infty} \frac{(-1)^n}{c^{n+2} n!} \frac{d^{n+1} \mathbf{u}}{dt^{n+1}} \int_V d^3 r \int_V d^3 r' \rho(r) R^{n-1} \rho(r'). \quad (10.143)$$

Distance R cancels only in the term with $n = 1$,

$$\mathbf{F}_1 = \frac{2}{3c^3} \frac{\ddot{\mathbf{u}}}{4\pi\epsilon_0} \int_V d^3 r \int_V d^3 r' \rho(r) \rho(r') = \frac{q^2}{6\pi\epsilon_0 c^3} \ddot{\mathbf{u}}, \quad (10.144)$$

and we see that we have recovered (now *apparently* in a legitimate fashion) Eq. (135) for the Abrahams-Lorentz force. One could argue that in the limit $a \rightarrow 0$ the terms higher in $R \sim a$ (with $n > 1$) could be ignored. However, we have to notice that the main contribution to \mathbf{F}_{self} is not (144), but the term with $n = 0$:

⁴⁷ Note: this is *not* a quantum spread due to the finite extent of the wavefunction. In quantum mechanics, parts of wavefunction of the same charged particle do *not* interact with each other!

$$\mathbf{F}_0 = -\frac{2}{3} \frac{1}{4\pi\epsilon_0} \frac{\dot{\mathbf{u}}}{c^2} \int_V d^3r \int_V d^3r' \frac{\rho(r)\rho(r')}{R} = -\frac{4}{3} \frac{\dot{\mathbf{u}}}{c^2} \frac{1}{8\pi\epsilon_0} \int_V d^3r \int_V d^3r' \frac{\rho(r)\rho(r')}{R} = -\frac{4}{3c^2} \dot{\mathbf{u}}U, \quad (10.145)$$

which may be interpreted as the inertial “force” with the effective *electromagnetic mass*

$$m_{\text{ef}} = \frac{4}{3} \frac{U}{c^2}. \quad (10.146)$$

This is the famous (or rather infamous :-)) *4/3 problem* which does not allow to interpret the electron’s mass as that of its electric field. The (admittedly, very formal) resolution of this paradox is possible only in quantum electrodynamics with its renormalization techniques, beyond the framework of this course. Notice that these issues are only important for motions with frequencies of the order of $1/\tau \sim 10^{23} \text{ s}^{-1}$, i.e. at energies $\mathcal{E} \sim \hbar/\tau \sim 10^{-11} \text{ J} \sim 10^8 \text{ eV}$, while other quantum electrodynamics effects may be observed at much lower frequencies, starting from $\sim 10^{10} \text{ s}^{-1}$. Hence the 4/3 problem is by no means the only motivation for the transfer from classical to quantum electrodynamics.

However, the reader should not think that his or her time spent on this course has been lost: the quantum electrodynamics incorporates virtually all of classical electrodynamics results, and transition between them is surprisingly straightforward.⁴⁸

⁴⁸ See, e.g., QM Chapter 8 and references therein.